Received November 8, 2015, accepted December 10, 2015, date of publication December 17, 2015, date of current version December 28, 2015.

Digital Object Identifier 10.1109/ACCESS.2015.2509449

Design and Optimal Configuration of Full-Duplex MAC Protocol for Cognitive Radio Networks Considering Self-Interference

LE THANH TAN[1], (Member, IEEE), AND LONG BAO LE[2], (Senior Member, IEEE)
[1]Department of Electrical Engineering, École Polytechnique de Montréal, Montréal, QC H3C 3A7, Canada
[2]Institut National de la Recherche Scientifique-Énergie, Matériaux et Télécommunications, Université du Québec, Montréal, QC H5A 1K6, Canada

Corresponding author: L. B. Le (long.le@emt.inrs.ca)

ABSTRACT In this paper, we propose an adaptive medium access control (MAC) protocol for full-duplex (FD) cognitive radio networks in which FD secondary users (SUs) perform channel contention followed by concurrent spectrum sensing and transmission, and transmission only with maximum power in two different stages (called the FD sensing and transmission stages, respectively) in each contention and access cycle. The proposed FD cognitive MAC (FDC-MAC) protocol does not require synchronization among SUs, and it efficiently utilizes the spectrum and mitigates the self-interference in the FD transceiver. We develop a mathematical model to analyze the throughput performance of the FDC-MAC protocol, where both half-duplex (HD) transmission and FD transmission modes are considered in the transmission stage. Then, we study the FDC-MAC configuration optimization through adaptively controlling the spectrum sensing duration and transmit power level in the FD sensing stage. We prove that there exists optimal sensing time and transmit power to achieve the maximum throughput, and we develop an algorithm to configure the proposed FDC-MAC protocol. Extensive numerical results are presented to illustrate the optimal FDC-MAC configuration and the impacts of protocol parameters and the self-interference cancellation quality on the throughput performance. Moreover, we demonstrate the significant throughput gains of the FDC-MAC protocol with respect to the existing HD MAC and single-stage FD MAC protocols.

INDEX TERMS Asynchronous MAC, full-duplex MAC, full-duplex spectrum sensing, optimal sensing duration, throughput maximization, self-interference control, full-duplex cognitive radios, throughput analysis.

I. INTRODUCTION

Engineering MAC protocols for efficient sharing of white spaces is an important research topic in cognitive radio networks (CRNs). One critical requirement for the cognitive MAC design is that transmissions on the licensed frequency band from primary users (PUs) should be satisfactorily protected from the SUs' spectrum access. Therefore, a cognitive MAC protocol for the secondary network must realize both the spectrum sensing and access functions so that timely detection of the PUs' communications and effective spectrum sharing among SUs can be achieved. Most existing research works on cognitive MAC protocols have focused on the design and analysis of HD MAC (e.g., see [1]–[4] and the references therein).

Due to the HD constraint, SUs typically employ a two-stage sensing/access procedure where they perform spectrum sensing in the first stage before accessing available spectrum for data transmission in the second stage [5]–[11]. The HD constraint also requires SUs be synchronized during the spectrum sensing stage, which could be difficult to achieve in practice. In fact, spectrum sensing enables SUs to detect white spaces that are not occupied by PUs [2]–[8], [12], [13]; therefore, imperfect spectrum sensing can reduce the spectrum utilization due to failure in detecting white spaces and potentially result in collisions with active PUs. Consequently, sophisticated design and parameter configuration of cognitive MAC protocols must be conducted to achieve good performance while appropriately protecting PUs [1], [6]–[11], [14]. As a result, traditional MAC protocols [15]–[19] adapted to the CRN may not provide satisfactory performance.

In general, HD MAC protocols may not exploit white spaces very efficiently since significant sensing time may be required, which would otherwise be utilized for data

2169-3536 © 2015 IEEE. Translations and content mining are permitted for academic research only.
Personal use is also permitted, but republication/redistribution requires IEEE permission.
See http://www.ieee.org/publications_standards/publications/rights/index.html for more information.

transmission. Moreover, SUs may not timely detect the PUs' activity during their transmissions, which can cause severe interference to active PUs. Thanks to recent advances on FD technologies, a FD radio can transmit and receive data simultaneously on the same frequency band [20]–[25]. In fact, the FD technology can be integrated into next-generation wireless networks, e.g., small cell networks and heterogeneous wireless networks [26], [27], to significantly enhance the network performance. One of the most critical issues of wireless FD communication is the presence of self-interference, which is caused by power leakage from the transmitter to the receiver of a FD transceiver. The self-interference may indeed lead to serious communication performance degradation of FD wireless systems. Despite recent advances on self-interference cancellation (SIC) techniques [21]–[23] (e.g., propagation SIC, analog-circuit SIC, and digital baseband SIC), self-interference still exists due to various reasons such as the limitation of hardware and channel estimation errors.

A. RELATED WORKS

There are some recent works that propose to exploit the FD communications for MAC-level channel access in multi-user wireless networks [25]–[31]. In [25], the authors develop a centralized MAC protocol to support asymmetric data traffic where network nodes may transmit data packets of different lengths, and they propose to mitigate the hidden node problem by employing a busy tone. To overcome this hidden node problem, Duarte et al. propose to adapt the standard 802.11 MAC protocol with the RTS/CTS handshake in [28]. Moreover, Goyal et al. in [29] extend this study to consider interference between two nodes due to their concurrent transmissions. Different from conventional wireless networks, designing MAC protocols in CRNs is more challenging because the spectrum sensing function must be efficiently integrated into the MAC protocol. In addition, the self-interference must be carefully addressed in the simultaneous spectrum sensing and access to mitigate its negative impacts on the sensing and throughput performance.

The FD technology has been employed for more efficient spectrum access design in cognitive radio networks [32]–[35] where SUs can perform sensing and transmission simultaneously. In [32], a FD MAC protocol is developed which allows simultaneous spectrum access of the SU and PU networks where both PUs and SUs are assumed to employ the p-persistent MAC protocol for channel contention resolution and access. This design is, however, not applicable to the hierarchical spectrum access in the CRNs where PUs should have higher spectrum access priority compared to SUs.

In our previous work [33], we propose the FD MAC protocol by using the standard backoff mechanism as in the 802.11 MAC protocol where we employ concurrent FD sensing and access during the data transmission phase as well as frame fragmentation. Moreover, engineering of a cognitive FD relaying network is considered in [34] and [35], where various resource allocation algorithms to improve the outage probability are proposed. In addition, the authors in [30] develop the joint routing and distributed resource allocation for FD wireless networks. In [31], Choi et al. study the distributed power allocation for a hybrid FD/HD system where all network nodes operate in the HD mode but the access point (AP) communicates by using the FD mode. In practice, it would be desirable to design an adaptable MAC protocol, which can be configured to operate in an optimal fashion depending on specific channel and network conditions. This design will be pursued in our current work.

B. OUR CONTRIBUTIONS

In this paper, we make a further bold step in designing, analyzing, and optimizing an adaptive FDC–MAC protocol for CRNs, where the self-interference and imperfect spectrum sensing are explicitly considered. In particular, the contributions of this paper can be summarized as follows.

1) We propose a novel FDC–MAC protocol that can efficiently exploit the FD transceiver for spectrum sensing and access of the white space without requiring synchronization among SUs. In this protocol, after the p-persistent based channel contention phase, the winning SU enters the data phase consisting of two stages, i.e., concurrent sensing and transmission in the first stage (called FD sensing stage) and transmission only in the second stage (called transmission stage). The developed FDC–MAC protocol, therefore, enables the optimized configuration of transmit power level and sensing time during the FD sensing stage to mitigate the self-interference and appropriately protect the active PU. After the FD sensing stage, the SU can transmit with the maximum power to achieve the highest throughput.
2) We develop a mathematical model for throughput performance analysis of the proposed FDC-MAC protocol considering the imperfect sensing, self-interference effects, and the dynamic status changes of the PU. In addition, both one-way and two-way transmission scenarios, which are called HD transmission (HDTx) and FD transmission (FDTx) modes, respectively, are considered in the analysis. Since the PU can change its idle/active status during the FD sensing and transmission stages, different potential status-change scenarios are studied in the analytical model.
3) We study the optimal configuration of FDC-MAC protocol parameters including the SU's sensing duration and transmit power to maximize the achievable throughput under both FDTx and HDTx modes. We prove that there exists an optimal sensing time to achieve the maximum throughput for a given transmit power value during the FD sensing stage under both FDTx and HDTx modes. Therefore, optimal protocol

parameters can be determined through standard numerical search methods.

4) Extensive numerical results are presented to illustrate the impacts of different protocol parameters on the throughput performance and the optimal configurations of the proposed FDC-MAC protocol. Moreover, we show the significant throughput enhancement of the proposed FDC-MAC protocol compared to existing cognitive MAC protocols, namely the HD MAC protocol and a single-stage FD MAC protocol with concurrent sensing and access during the whole data phase. Specifically, our FDC-MAC protocol achieves higher throughput with the increasing maximum power while the throughput of the single-stage FD MAC protocol decreases with the maximum power in the high power regime due to the self-interference. Moreover, the proposed FDC-MAC protocol significantly outperforms the HD MAC protocol in terms of system throughput.

The remaining of this paper is organized as follows. Section II describes the system and PU models. FDC–MAC protocol design, and throughput analysis are performed in Section III. Then, Section IV studies the optimal configuration of the proposed FDC–MAC protocol. Section V demonstrates numerical results followed by concluding remarks in Section VI.

II. SYSTEM AND PU ACTIVITY MODELS

A. SYSTEM MODEL

We consider a cognitive radio network where n_0 pairs of SUs opportunistically exploit white spaces on one channel for communications. We assume that each SU is equipped with a FD transceiver; hence, the SUs can perform sensing and transmission simultaneously. However, the sensing performance of each SU is affected by the self-interference from its transmitter since the transmitted power is leaked into the received signal. We denote $I(P)$ as the average self-interference power, which is modeled as $I(P) = \zeta\,(P)^{\xi}$ [20] where P is the SU's transmit power, ζ and ξ $(0 \leq \xi \leq 1)$ are predetermined coefficients which represent the quality of self-interference cancellation (QSIC). In this work, we design an asynchronous cognitive MAC protocol where no synchronization is required among SUs and between SUs and the PU. We assume that different pairs of SUs can overhear transmissions from the others (i.e., a collocated network is assumed). In the following, we refer to pair i of SUs as SU i for brevity.

B. PRIMARY USER ACTIVITY

We assume that the PU's idle/active status follows two independent random processes. We say that the channel is available and busy for SUs' access if the PU is in the idle and active (or busy) states, respectively. Let $\mathcal{H}_0$ and $\mathcal{H}_1$ denote the events that the PU is idle and active, respectively. To protect the PU, we assume that SUs must stop their transmissions and evacuate from the busy channel within the maximum delay of T_{eva}, which is referred to as channel evacuation time.

Let τ_{ac} and τ_{id} denote the random variables which represent the durations of active and idle channel states, respectively. We denote probability density functions (pdf) of τ_{ac} and τ_{id} as $f_{\tau_{\text{ac}}}(t)$ and $f_{\tau_{\text{id}}}(t)$, respectively. While most results in this paper can be applied to general pdfs $f_{\tau_{\text{ac}}}(t)$ and $f_{\tau_{\text{id}}}(t)$, we mostly consider the exponential pdf in the analysis. In addition, let $\mathcal{P}(\mathcal{H}_0) = \frac{\bar{\tau}_{\text{id}}}{\bar{\tau}_{\text{id}}+\bar{\tau}_{\text{ac}}}$ and $\mathcal{P}(\mathcal{H}_1) = 1 - \mathcal{P}(\mathcal{H}_0)$ present the probabilities that the channel is available and busy, respectively where $\bar{\tau}_{\text{id}}$ and $\bar{\tau}_{\text{ac}}$ denote the average values of τ_{ac} and τ_{id}, respectively. We assume that the probabilities that τ_{ac} and τ_{id} are smaller than T_{eva} are sufficiently small (i.e., the PU changes its status slowly) so that we can ignore events with multiple idle/active status changes in one channel evacuation interval T_{eva}.

III. FULL-DUPLEX COGNITIVE MAC PROTOCOL

In this section, we describe the proposed FDC-MAC protocol and conduct its throughput analysis considering imperfect sensing, self-interference of the FD transceiver, and dynamic status change of the PUs.

A. FDC-MAC PROTOCOL DESIGN

The proposed FDC-MAC protocol integrates three important elements of a cognitive MAC protocol, namely contention resolution, spectrum sensing, and access functions. Specifically, SUs employ the p-persistent CSMA principle [17] for contention resolution where each SU with data to transmit attempts to capture an available channel with a probability p after the channel is sensed to be idle during the standard DIFS interval (DCF Interframe Space). If a particular SU decides not to transmit (with probability of $1 - p$), it will sense the channel and attempt to transmit again in the next slot of length σ with probability p. To complete the reservation, the four-way handshake with Request-to-Send/Clear-to-Send (RTS/CST) exchanges [16] is employed to reserve the available channel for transmission. Specifically, the secondary transmitter sends RTS to the secondary receiver and waits until it successfully receives the CTS from the secondary receiver. All other SUs, which hear the RTS and CTS exchange from the winning SU, defer to access the channel for a duration equal to the data transmission time, T. Then, an acknowledgment (ACK) from the SU's receiver is transmitted to its corresponding transmitter to notify the successful reception of a packet. Furthermore, the standard small interval, namely SIFS (Short Interframe Space), is used before the transmissions of CTS, ACK, and data frame as in the standard 802.11 MAC protocol [16].

In our design, the data phase after the channel contention phase comprises two stages where the SU performs concurrent sensing and transmission in the first stage with duration T_S and transmission only in the second stage with duration $T - T_S$. Here, the SU exploits the FD capability of its transceiver to realize concurrent sensing and transmission

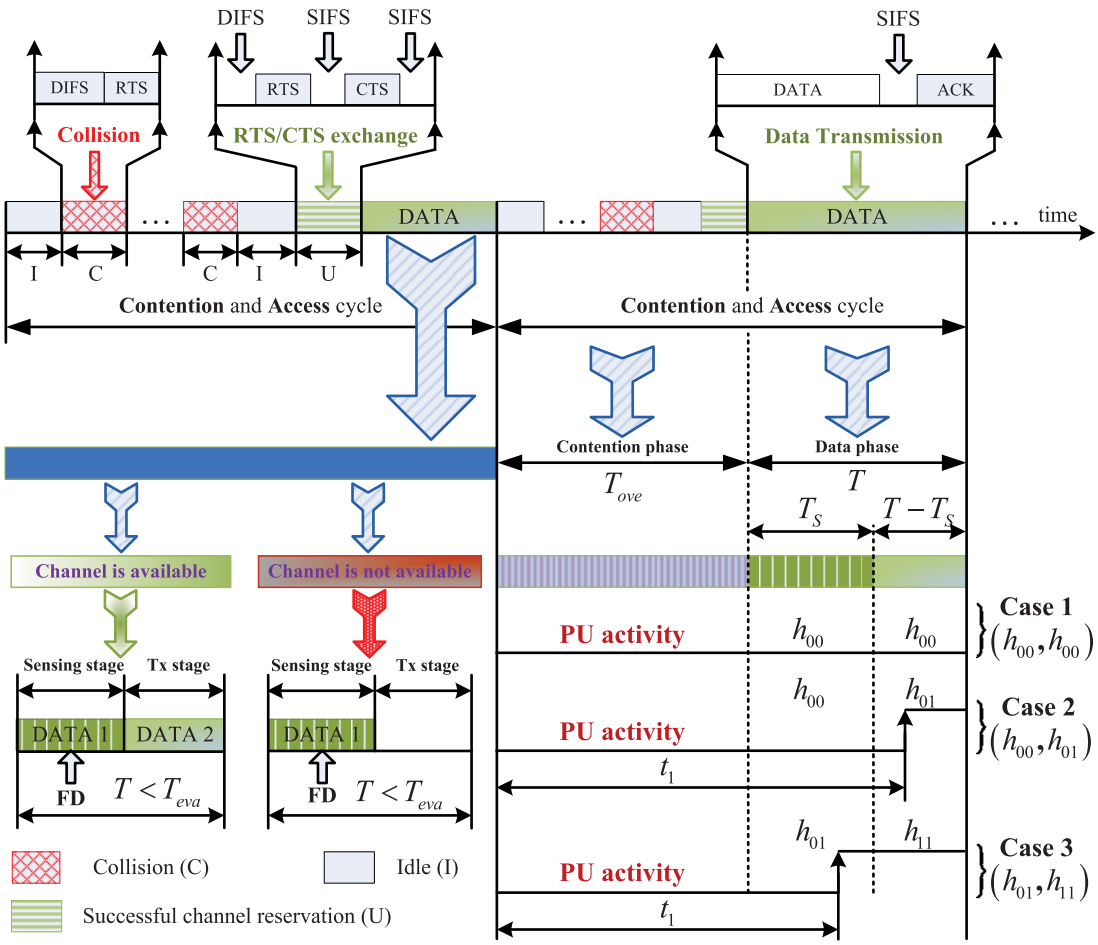

FIGURE 1. Timing diagram of the proposed full-duplex cognitive MAC protocol.

the first stage (called FD sensing stage) where the sensing outcome at the end of this stage (i.e., an idle or busy channel status) determines its further actions as follows. Specifically, if the sensing outcome indicates an available channel then the SU transmits data in the second stage; otherwise, it remains silent for the remaining time of the data phase with duration $T - T_S$.

We assume that the duration of the SU's data phase T is smaller than the channel evacuation time T_{eva} so timely evacuation from the busy channel can be realized with reliable FD spectrum sensing. Therefore, our design allows to protect the PU with evacuation delay at most T if the MAC carrier sensing during the contention phase and the FD spectrum sensing in the data phase are perfect. Furthermore, we assume that the SU transmits at power levels $P_{\text{sen}} \leq P_{\text{max}}$ and $P_{\text{dat}} = P_{\text{max}}$ during the FD sensing and transmission stages, respectively where P_{max} denotes the maximum power and the transmit power P_{sen} in the FD sensing stage will be optimized to effectively mitigate the self-interference and achieve good sensing-throughput tradeoff. The timing diagram of the proposed FDC–MAC protocol is illustrated in Fig. 1.

We allow two possible operation modes in the transmission stage. The first is the HD transmission mode (HDTx mode) where there is only one direction of data transmission from the SU transmitter to the SU receiver. In this mode, there is no self-interference in the transmission stage. The second is the FD transmission mode (FDTx mode) where two-way communications between the pair of SUs are assumed (i.e., there are two data flows between the two SU nodes in opposite directions). In this mode, the achieved throughput can be potentially enhanced (at most doubling the throughput of the HDTx mode) but self-interference must be taken into account in throughput quantification.

Our proposed FDC–MAC protocol design indeed enables flexible and adaptive configuration, which can efficiently exploit the capability of the FD transceiver. Specifically, if the duration of the FD sensing stage is set equal to the duration of the whole data phase (i.e., $T_S = T$), then the SU performs concurrent sensing and transmission for the whole data phase as in our previous design [33]. This configuration may degrade the achievable throughput since the transmit power during the FD sensing stage is typically set smaller P_{max} to mitigate the self-interference and achieve the required

sensing performance. We will refer the corresponding MAC protocol with $T_S = T$ as one-stage FD MAC in the sequel.

Moreover, if we set the SU transmit power P_{sen} in the sensing stage equal to zero, i.e., $P_{\text{sen}} = 0$, then we achieve the traditional two-stage cognitive HD MAC protocol where sensing and transmission are performed sequentially in two different stages [6], [8]. Moreover, the proposed FDC–MAC protocol is more flexible than existing designs [6], [8], [33] since different existing designs can be achieved through suitable configuration of its protocol parameters. It will be demonstrated later that the proposed FDC–MAC protocol achieves significant better throughput than that of the existing cognitive MAC protocols. In the following, we present the throughput analysis based on which the protocol configuration optimization can be performed.

B. THROUGHPUT ANALYSIS

We now conduct the saturation throughput analysis for the secondary network where all SUs are assumed to always have data to transmit. The resulting throughput can be served as an upper bound for the throughput in the non-saturated scenario [16]. This analysis is performed by studying one specific contention and access cycle (CA cycle) with the contention phase and data phase as shown in Fig. 1. Without loss of generality, we will consider the normalized throughput achieved per one unit of system bandwidth (in bits/s/Hz). Specifically, the normalized throughput of the FDC–MAC protocol can be expressed as

$$\mathcal{NT} = \frac{\mathcal{B}}{T_{\text{ove}} + T}, \tag{1}$$

where T_{ove} represents the time overhead required for one successful channel reservation (i.e., successful RTS/CTS exchanges), T denotes the packet transmission time, and $\mathcal{B}$ denotes the amount of data (bits) transmitted in one CA cycle per one unit of system bandwidth, which is expressed in bits/Hz. To complete the throughput analysis, we derive the quantities T_{ove} and $\mathcal{B}$ in the remaining of this subsection.

1) DERIVATION OF T_{ove}

The average time overhead for one successful channel reservation can be calculated as

$$T_{\text{ove}} = \overline{T}_{\text{cont}} + 2SIFS + 2PD + ACK, \tag{2}$$

where ACK is the length of an ACK message, $SIFS$ is the length of a short interframe space, and PD is the propagation delay where PD is usually small compared to the slot size σ, and $\overline{T}_{\text{cont}}$ denotes the average time overhead due to idle periods, collisions, and successful transmissions of RTS/CTS messages in one CA cycle. For better presentation of the paper, the derivation of $\overline{T}_{\text{cont}}$ is given in Appendix A.

2) DERIVATION OF $\mathcal{B}$

To calculate $\mathcal{B}$, we consider all possible cases that capture the activities of SUs and status changes of the PU in the FDC-MAC data phase of duration T. Because the PU's activity is not synchronized with the SU's transmission, the PU can change its idle/active status any time. We assume that there can be at most one transition between the idle and active states of the PU during one data phase interval. This is consistent with the assumption on the slow status changes of the PU as described in Section II-B since $T < T_{\text{eva}}$. Furthermore, we assume that the carrier sensing of the FDC-MAC protocol is perfect; therefore, the PU is idle at the beginning of the FDC-MAC data phase. Note that the PU may change its status during the SU's FD sensing or transmission stage, which requires us to consider different possible events in the data phase.

We use h_{ij} $(i, j \in \{0, 1\})$ to represent events capturing status changes of the PU in the FD sensing stage and transmission stage where $i = 0$ and $i = 1$ represent the idle and active states of the PU, respectively. For example, if the PU is idle during the FD sensing stage and becomes active during the transmission stage, then we represent this event as (h_{00}, h_{01}) where sub-events h_{00} and h_{01} represent the status changes in the FD sensing and transmission stages, respectively. Moreover, if the PU changes from the idle to the active state during the FD sensing stage and remains active in the remaining of the data phase, then we represent this event as (h_{01}, h_{11}).

It can be verified that we must consider the following three cases with the corresponding status changes of the PU during the FDC-MAC data phase to analyze $\mathcal{B}$.

- *Case 1:* The PU is idle for the whole FDC-MAC data phase (i.e., there is no PU's signal in both FD sensing and transmission stages) and we denote this event as (h_{00}, h_{00}). The average number of bits (in bits/Hz) transmitted during the data phase in this case is denoted as $\mathcal{B}_1$.
- *Case 2:* The PU is idle during the FD sensing stage but the PU changes from the idle to the active status in the transmission stage. We denote the event corresponding to this case as (h_{00}, h_{01}) where h_{00} and h_{01} capture the sub-events in the FD sensing and transmission stages, respectively. The average number of bits (in bits/Hz) transmitted during the data phase in this case is represented by $\mathcal{B}_2$.
- *Case 3:* The PU is first idle then becomes active during the FD sensing stage and it remains active during the whole transmission stage. Similarly we denote this event as (h_{01}, h_{11}) and the average number of bits (in bits/Hz) transmitted during the data phase in this case is denoted as $\mathcal{B}_3$.

Then, we can calculate $\mathcal{B}$ as follows:

$$\mathcal{B} = \mathcal{B}_1 + \mathcal{B}_2 + \mathcal{B}_3. \tag{3}$$

To complete the analysis, we will need to derive $\mathcal{B}_1$, $\mathcal{B}_2$, and $\mathcal{B}_3$, which are given in Appendix B.

IV. FDC–MAC PROTOCOL CONFIGURATION FOR THROUGHPUT MAXIMIZATION

In this section, we study the optimal configuration of the proposed FDC–MAC protocol to achieve the maximum throughput while satisfactorily protecting the PU.

A. PROBLEM FORMULATION

Let $\mathcal{NT}(T_S, p, P_{\text{sen}})$ denote the normalized secondary throughput, which is the function of the sensing time T_S, transmission probability p, and the SU's transmit power P_{sen} in the FD sensing stage. In the following, we assume a fixed frame length T, which is set smaller the required evacuation time T_{eva} to achieve timely evacuation from a busy channel for the SUs. We are interested in determining suitable configuration for p, T_S and P_{sen} to maximize the secondary throughput, $\mathcal{NT}(T_S, p, P_{\text{sen}})$. In general, the optimal transmission probability p should balance between reducing collisions among SUs and limiting the protocol overhead. However, the achieved throughput is less sensitive to the transmission probability p as will be demonstrated later via the numerical study. Therefore, we will seek to optimize the throughput over P_{sen} and T_S for a reasonable and fixed value of p.

For brevity, we express the throughput as a function of P_{sen} and T_S only, i.e., $\mathcal{NT}(T_S, P_{\text{sen}})$. Suppose that the PU requires that the average detection probability is at least $\overline{\mathcal{P}}_d$. Then, the throughput maximization problem can be stated as follows:

$$\begin{aligned} &\max_{T_S, P_{\text{sen}}} \ \mathcal{NT}(T_S, P_{\text{sen}}) \\ &\text{s.t. } \hat{\mathcal{P}}_d(\varepsilon, T_S) \geq \overline{\mathcal{P}}_d, \\ &\quad 0 \leq P_{\text{sen}} \leq P_{\text{max}}, \quad 0 \leq T_S \leq T, \end{aligned} \tag{4}$$

where P_{max} is the maximum power for SUs, and T_S is upper bounded by T. In fact, the first constraint on $\hat{\mathcal{P}}_d(\varepsilon, T_S)$ implies that the spectrum sensing should be sufficiently reliable to protect the PU which can be achieved with sufficiently large sensing time T_S. Moreover, the SU's transmit power P_{sen} must be appropriately set to achieve good tradeoff between the network throughput and self-interference mitigation.

B. PARAMETER CONFIGURATION FOR FDC–MAC PROTOCOL

To gain insights into the parameter configuration of the FDC–MAC protocol, we first study the optimization with respect to the sensing time T_S for a given P_{sen}. For any value of T_S, we would need to set the sensing detection threshold ε so that the detection probability constraint is met with equality, i.e., $\hat{\mathcal{P}}_d(\varepsilon, T_S) = \overline{\mathcal{P}}_d$ as in [5] and [6]. Since the detection probability is smaller in **Case 3** (i.e., the PU changes from the idle to active status during the FD sensing stage of duration T_S) compared to that in **Case 1** and **Case 2** (i.e., the PU remains idle during the FD sensing stage) considered in the previous section, we only need to consider **Case 3** to maintain the detection probability constraint. The average probability of detection for the FD sensing in **Case 3** can be expressed as

$$\hat{\mathcal{P}}_d = \int_0^{T_S} \mathcal{P}_d^{01}(t) f_{\tau_{\text{id}}}(t \,|0 \leq t \leq T_S)\, dt, \tag{5}$$

where t denotes the duration from the beginning of the FD sensing stage to the instant when the PU changes to the active state, and $f_{\tau_{\text{id}}}(t\,|\mathcal{A})$ is the pdf of τ_{id} conditioned on event $\mathcal{A}$ capturing the condition $0 \leq t \leq T_S$, which is given as

$$f_{\tau_{\text{id}}}(t\,|\mathcal{A}) = \frac{f_{\tau_{\text{id}}}(t)}{\Pr\{\mathcal{A}\}} = \frac{\frac{1}{\overline{\tau}_{\text{id}}} \exp(-\frac{t}{\overline{\tau}_{\text{id}}})}{1 - \exp(-\frac{T_S}{\overline{\tau}_{\text{id}}})}. \tag{6}$$

Note that $\mathcal{P}_d^{01}(t)$ is derived in Appendix C and $f_{\tau_{\text{id}}}(t)$ is given in (18).

We consider the following single-variable optimization problem for a given P_{sen}:

$$\max_{0 < T_S \leq T} \quad \mathcal{NT}(T_S, P_{\text{sen}}). \tag{7}$$

We characterize the properties of function $\mathcal{NT}(T_S, P_{\text{sen}})$ with respect to T_S for a given P_{sen} in the following theorem whose proof is provided in Appendix D. For simplicity, the throughput function is written as $\mathcal{NT}(T_S)$.

Theorem 1: The objective function $\mathcal{NT}(T_S)$ of (7) satisfies the following properties

1) $\lim_{T_S \to 0} \frac{\partial \mathcal{NT}}{\partial T_S} = +\infty$,
2) a) For HDTx mode with $\forall P_{\text{sen}}$ and FDTx mode with $P_{\text{sen}} < \overline{P}_{\text{sen}}$, we have $\lim_{T_S \to T} \frac{\partial \mathcal{NT}}{\partial T_S} < 0$,
   b) For FDTx mode with $P_{\text{sen}} > \overline{P}_{\text{sen}}$, we have $\lim_{T_S \to T} \frac{\partial \mathcal{NT}}{\partial T_S} > 0$,
3) $\frac{\partial^2 \mathcal{NT}}{\partial T_S^2} < 0, \forall T_S$,
4) The objective function $\mathcal{NT}(T_S)$ is bounded from above,

where $\overline{P}_{\text{sen}} = N_0 \left[\left(1 + \frac{P_{\text{dat}}}{N_0 + \zeta P_{\text{dat}}^{\xi}} \right)^2 - 1 \right]$ is the critical value of P_{sen} such that $\lim_{T_S \to T} \frac{\partial \mathcal{NT}}{\partial T_S} = 0$.

We would like to discuss the properties stated in Theorem 1. For the HDTx mode with $\forall P_{\text{sen}}$ and FDTx mode with low P_{sen}, then properties 1, 2a, and 4 imply that there must be at least one T_S in $[0, T]$ that maximizes $\mathcal{NT}(T_S)$. The third property implies that this maximum is indeed unique. Moreover, for the FDTx with high P_{sen}, then properties 1, 2b, 3 and 4 imply that $\mathcal{NT}(T_S)$ increases in $[0, T]$. Hence, the throughput $\mathcal{NT}(T_S)$ achieves its maximum with sensing time $T_S = T$. We propose an algorithm to determine optimal (T_S, P_{sen}), which is summarized in Algorithm 1. Here, we can employ the bisection scheme and other numerical methods to determine the optimal value T_S for a given P_{sen}.

Algorithm 1 FDC-MAC Configuration Algorithm

1: **for** each considered value of $P_{\text{sen}} \in [0, P_{\text{max}}]$ **do**
2: Find optimal T_S for problem (7) using the bisection method as $\overline{T}_S(P_{\text{sen}}) = \underset{0 \leq T_S \leq T}{\text{argmax}}\, \mathcal{NT}(T, P_{\text{sen}})$.
3: **end for**
4: The final solution $(T_S^*, P_{\text{sen}}^*)$ is determined as $(T_S^*, P_{\text{sen}}^*) = \underset{P_{\text{sen}}, \overline{T}_S(P_{\text{sen}})}{\text{argmax}}\, \mathcal{NT}(T_S(P_{\text{sen}}), P_{\text{sen}})$.

V. NUMERICAL RESULTS

For numerical studies, we set the key parameters for the FDC–MAC protocol as follows: mini-slot duration is $\sigma = 20\mu s$; $PD = 1\mu s$; $SIFS = 2\sigma\ \mu s$; $DIFS = 10\sigma\ \mu s$; $ACK = 20\sigma\ \mu s$; $CTS = 20\sigma\ \mu s$; $RTS = 20\sigma\ \mu s$. Other parameters are chosen as follows unless stated otherwise: the sampling frequency $f_s = 6$ MHz; bandwidth of PU's signal 6 MHz; $\overline{\mathcal{P}}_d = 0.8$; $T = 15$ ms; $p = 0.0022$; the SNR of the PU signal at each SU $\gamma_P = \frac{P_p}{N_0} = -20$ dB; varying self-interference parameters ζ and ξ. Without loss of generality, the noise power is normalized to one; hence, the SU transmit power P_{sen} becomes $P_{\text{sen}} = SNR_s$; and we set $P_{\text{max}} = 15$dB.

We first study the impacts of self-interference parameters on the throughput performance with the following parameter setting: $(\bar{\tau}_{\text{id}}, \bar{\tau}_{\text{ac}}) = (1000, 100)$ ms, $P_{\text{max}} = 25$ dB, $T_{\text{eva}} = 40$ ms, $\zeta = 0.4$, ξ is varied in $\xi = \{0.12, 0.1, 0.08, 0.05\}$, and $P_{\text{dat}} = P_{\text{max}}$. Recall that the self-interference depends on the transmit power P as $I(P) = \zeta\,(P)^{\xi}$ where $P = P_{\text{sen}}$ and $P = P_{\text{dat}}$ in the FD sensing and transmission stages, respectively. Fig. 2 illustrates the variations of the throughput versus the transmission probability p. It can be observed that when ξ decreases (i.e., the self-interference is smaller), the achieved throughput increases. This is because SUs can transmit with higher power while still maintaining the sensing constraint during the FD sensing stage, which leads to throughput improvement. The optimal P_{sen} corresponding to these values of ξ are $P_{\text{sen}} = SNR_s = \{25.00, 18.01, 14.23, 11.28\}$ dB and the optimal probability of transmission is $p^* = 0.0022$ as indicated by a star symbol. Therefore, to obtain all other results in this section, we set $p^* = 0.0022$.

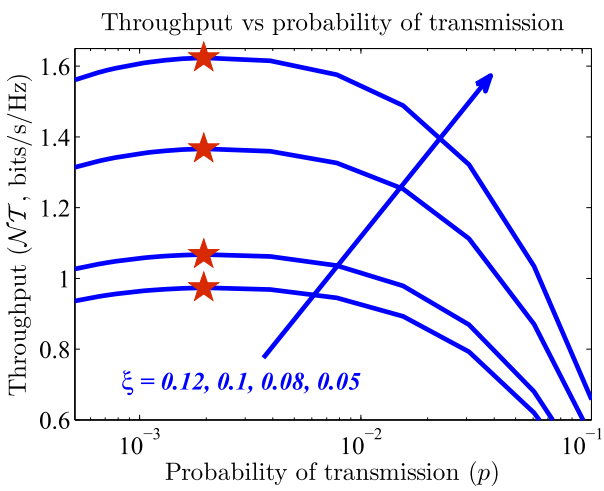

FIGURE 2. Normalized throughput versus transmission probability p for $T = 18$ ms, $\bar{\tau}_{\text{id}} = 1000$ ms, $\bar{\tau}_{\text{ac}} = 100$ ms, and varying ξ.

Fig. 3 illustrates the throughput performance versus number of SUs n_0 when we keep the same parameter settings as those for Fig. 2 and $p^* = 0.0022$. Again, when ξ decreases (i.e., the self-interference becomes smaller), the achieved throughput increases. In this figure, the optimal

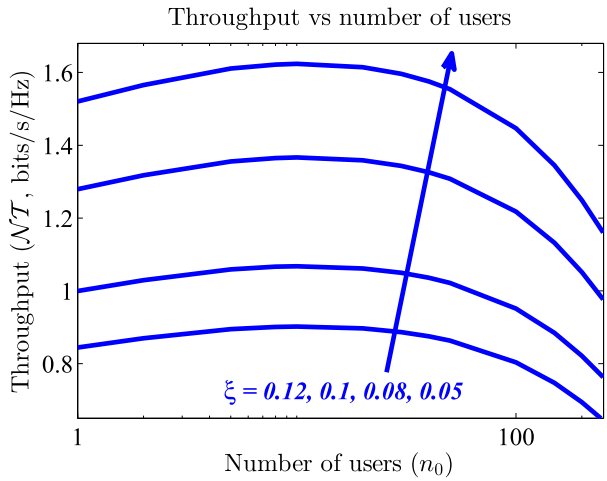

FIGURE 3. Normalized throughput versus the number of SUs n_0 for $T = 18$ ms, $p = 0.0022$, $\bar{\tau}_{\text{id}} = 1000$ ms, $\bar{\tau}_{\text{ac}} = 100$ ms, and varying ξ.

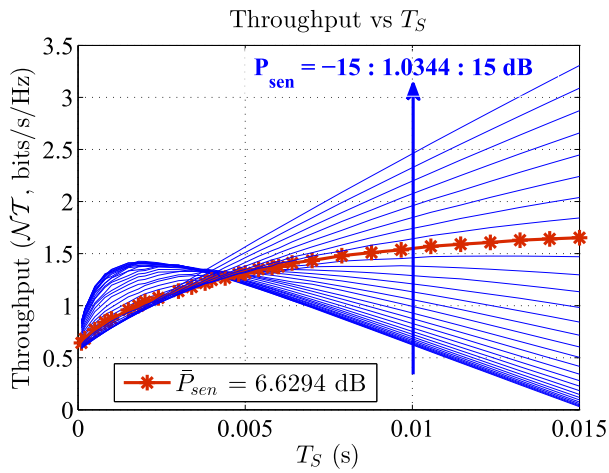

FIGURE 4. Normalized throughput versus SU transmit power P_{sen} and sensing time T_S for $p = 0.0022$, $\bar{\tau}_{\text{id}} = 500$ ms, $\bar{\tau}_{\text{ac}} = 50$ ms, $n_0 = 40$, $\xi = 1$, $\zeta = 0.7$ and FDTx with $P_{\text{dat}} = 15$ dB.

SNR_s achieving the maximum throughput corresponding to the considered values of ξ are $P_{\text{sen}} = SNR_s = \{25.00, 18.01, 14.23, 11.28\}$ dB, respectively.

We now verify the results stated in Theorem 1 for the FDTx mode. Specifically, Fig. 4 shows the throughput performance for the scenario where the QSIC is very low with large ξ and ζ where we set the network parameters as follows: $p = 0.0022$, $\bar{\tau}_{\text{id}} = 500$ ms, $\bar{\tau}_{\text{ac}} = 50$ ms, $n_0 = 40$, $\xi = 1$, $\zeta = 0.7$, and $P_{\text{dat}} = 15$ dB. Moreover, we can obtain $\overline{P}_{\text{sen}}$ as in (42) in Appendix D, which is equal to $\overline{P}_{\text{sen}} = 6.6294$ dB. In this figure, the curve indicated by asterisks, which corresponds to $P_{\text{sen}} = \overline{P}_{\text{sen}}$, shows the monotonic increase of the throughput with sensing time T_S and other curves corresponding to $P_{\text{sen}} > \overline{P}_{\text{sen}}$ have the same characteristic. In contrast, all remaining curves (corresponding to $P_{\text{sen}} < \overline{P}_{\text{sen}}$) first increase to the maximum values and then decrease as we increase T_S.

Fig. 5 illustrates the throughput performance for the very high QSIC with small ξ and ζ where we set the network

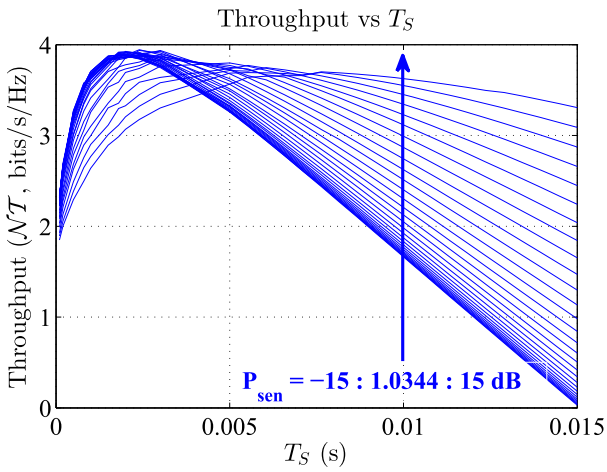

FIGURE 5. Normalized throughput versus SU transmit power P_{sen} and sensing time T_S for $p = 0.0022$, $\bar{\tau}_{\text{id}} = 500$ ms, $\bar{\tau}_{\text{ac}} = 50$ ms, $n_0 = 40$, $\xi = 1$, $\zeta = 0.08$ and FDTx with $P_{\text{dat}} = 15$ dB.

parameters as follows: $p = 0.0022$, $\bar{\tau}_{\text{id}} = 500$ ms, $\bar{\tau}_{\text{ac}} = 50$ ms, $n_0 = 40$, $\xi = 1$, $\zeta = 0.08$, and $P_{\text{dat}} = 15$ dB. Moreover, we can obtain $\overline{P}_{\text{sen}}$ as in (42) in Appendix D, which is equal to $\overline{P}_{\text{sen}} = 19.9201$ dB. We have $P_{\text{sen}} < P_{\text{max}} = 15dB < \overline{P}_{\text{sen}}$ in this scenario; hence, all the curves first increases to the maximum throughput and then decreases with the increasing T_S. Therefore, we have correctly validated the properties stated in Theorem 1.

Now we investigate the throughput performance versus SU transmit power P_{sen} and sensing time T_S for the case of high QSIC with $\xi = 0.95$ and $\zeta = 0.08$. Fig. 6 shows the throughput versus the SU transmit power P_{sen} and sensing time T_S for the FDTx mode with $P_{\text{dat}} = 15$ dB, $p = 0.0022$, $\bar{\tau}_{\text{id}} = 150$ ms, $\bar{\tau}_{\text{ac}} = 50$ ms, and $n_0 = 40$. It can be observed that there exists an optimal configuration of the SU transmit power $P^*_{\text{sen}} = 4.6552$ dB and sensing time $T^*_S = 2.44$ ms to

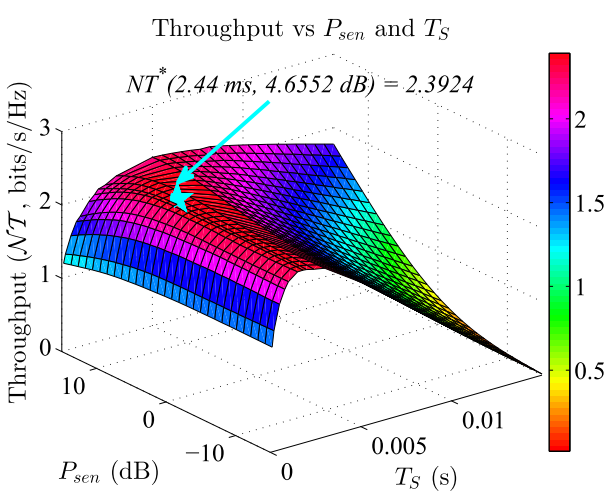

FIGURE 6. Normalized throughput versus SU transmit power P_{sen} and sensing time T_S for $p = 0.0022$, $\bar{\tau}_{\text{id}} = 150$ ms, $\bar{\tau}_{\text{ac}} = 50$ ms, $n_0 = 40$, $\xi = 0.95$, $\zeta = 0.08$ and FDTx with $P_{\text{dat}} = 15$ dB.

achieve the maximum throughput $\mathcal{NT}\left(T^*_S, P^*_{\text{sen}}\right) = 2.3924$, which is indicated by a star symbol. These results confirm that SUs must set appropriate sensing time and transmit power for the FDC–MAC protocol to achieve the maximize throughput, which cannot be achieved by setting $T_s = T$ as proposed in existing designs such as in [33].

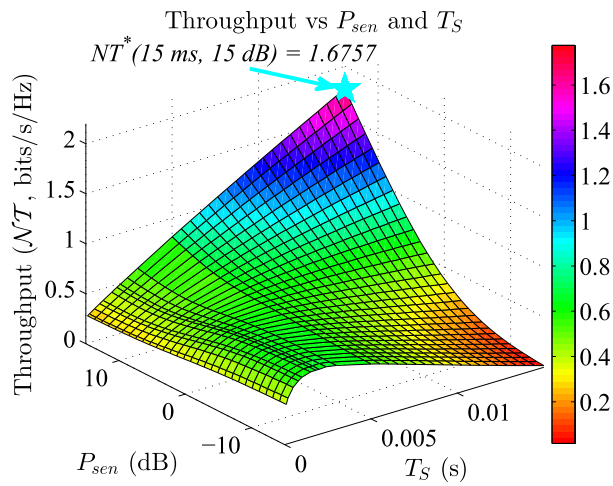

FIGURE 7. Normalized throughput versus SU transmit power P_{sen} and sensing time T_S for $p = 0.0022$, $\bar{\tau}_{\text{id}} = 150$ ms, $\bar{\tau}_{\text{ac}} = 50$ ms, $n_0 = 40$, $\xi = 0.95$, $\zeta = 0.8$ and FDTx with $P_{\text{dat}} = 15$ dB.

In Fig. 7, we present the throughput versus the SU transmit power P_{sen} and sensing time T_S for the low QSIC scenario where $p = 0.0022$, $\bar{\tau}_{\text{id}} = 150$ ms, $\bar{\tau}_{\text{ac}} = 50$ ms, $P_{\text{max}} = 15$ dB, $n_0 = 40$, $\xi = 0.95$, and $\zeta = 0.8$. The optimal configuration of SU transmit power $P^*_{\text{sen}} = 15$ dB and sensing time $T^*_S = 15$ ms to achieve the maximum throughput $\mathcal{NT}\left(T^*_S, P^*_{\text{sen}}\right) = 1.6757$ is again indicated by a star symbol. Under this optimal configuration, the FD sensing is performed during the whole data phase (i.e., there is no transmission stage). In fact, to achieve the maximum throughput, the SU must provide the satisfactory sensing performance and attempt to achieve high transmission rate. Therefore, if the QSIC is low, the data rate achieved during the transmission stage can be lower than that in the FD sensing stage because of the very strong self-interference in the transmission stage. Therefore, setting longer FD sensing time enables to achieve more satisfactory sensing performance and higher transmission rate, which explains that the optimal configuration should set $T^*_S = T$ for the low QSIC scenario. This protocol configuration corresponds to existing design in [33], which is a special case of the proposed FDC–MAC protocol.

We now investigate the throughput performance with respect to the SU transmit power P_{sen} and sensing time T_S for the HDTx mode. Fig. 8 illustrates the throughput performance for the high QSIC scenario with $\xi = 0.95$ and $\zeta = 0.08$. It can be observed that there exists an optimal configuration of SU transmit power $P^*_{\text{sen}} = 5.6897$ dB and sensing time $T^*_S = 3.5$ ms to achieve the maximum throughput $\mathcal{NT}\left(T^*_S, P^*_{\text{sen}}\right) = 1.4802$, which is indicated

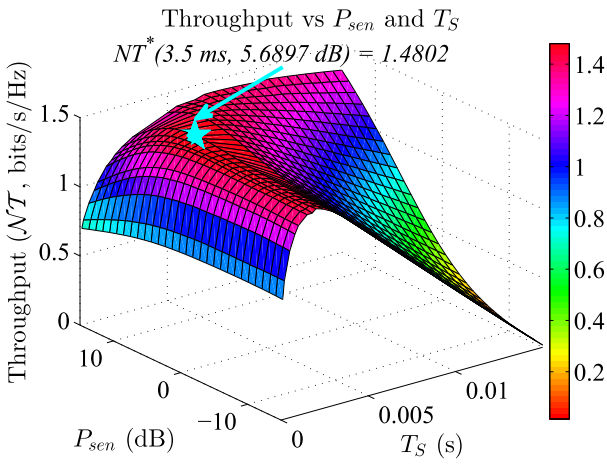

FIGURE 8. Normalized throughput versus SU transmit power P_{sen} and sensing time T_S for $p = 0.0022$, $\bar{\tau}_{\text{id}} = 150$ ms, $\bar{\tau}_{\text{ac}} = 50$ ms, $n_0 = 40$, $\xi = 0.95$, $\zeta = 0.08$ and HDTx.

by a star symbol. The maximum achieved throughput of the HDTx mode is lower than that in the FDTx mode presented in Fig. 6. This is because with high QSIC, the FDTx mode can transmit more data than the HDTx mode in the transmission stage.

In Fig. 9, we show the throughput versus the SU transmit power P_{sen} for $T_S = 2.2$ ms, $p = 0.0022$, $\bar{\tau}_{\text{id}} = 1000$ ms, $\bar{\tau}_{\text{ac}} = 50$ ms, $n_0 = 40$, $\xi = 0.95$, $\zeta = 0.08$ and various values of T (i.e., the data phase duration) for the FDTx mode with $P_{\text{dat}} = 15$ dB. For each value of T, there exists the optimal SU transmit power P^*_{sen} which is indicated by an asterisk. It can be observed that as T increases from 8 ms to 25 ms, the achieved maximum throughput first increases then decreases with T. Also in the case with $T^* = 15$ ms, the SU achieves the largest throughput which is indicated by a star symbol. Furthermore, the achieved throughput significantly decreases when the pair of (T, P_{sen}) deviates from the optimal values, (T^*, P^*_{sen}).

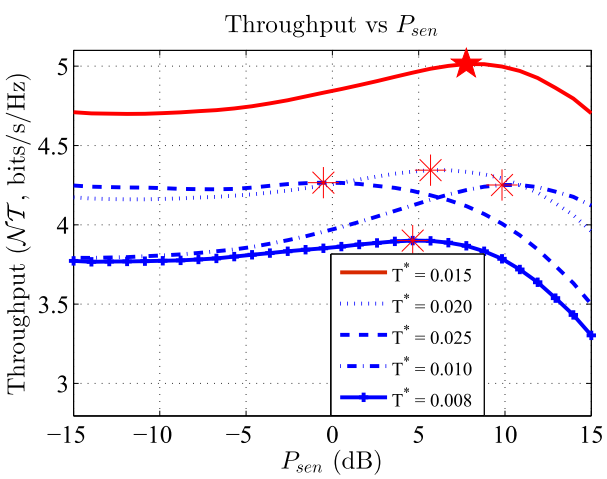

FIGURE 9. Normalized throughput versus SU transmit power P_{sen} for $T_S = 2.2$ ms, $p = 0.0022$, $\bar{\tau}_{\text{id}} = 1000$ ms, $\bar{\tau}_{\text{ac}} = 50$ ms, $n_0 = 40$, $\xi = 0.95$, $\zeta = 0.08$, varying T, and FDTx with $P_{\text{dat}} = 15$ dB.

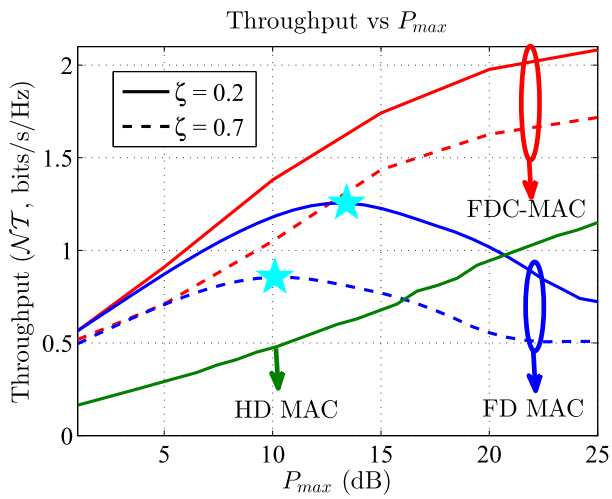

FIGURE 10. Normalized throughput versus P_{max} for $\bar{\tau}_{\text{id}} = 150$ ms, $\bar{\tau}_{\text{ac}} = 75$ ms, $n_0 = 40$, $\xi = 0.85$, $n_0 = 40$, $\zeta = \{0.2, 0.7\}$, and FDTx with $P_{\text{dat}} = P_{\text{max}}$ dB.

Finally, we compare the throughput of our proposed FDC-MAC protocol, the single-stage FD MAC protocol where FD sensing (concurrent spectrum sensing and transmission) is performed during the whole data phase [33] and the HD MAC protocol which does not allow the transmission during the spectrum sensing interval in Fig. 10. For brevity, the single-stage FD MAC protocol is refereed to as FD MAC in this figure. The parameter settings are as follows: $\bar{\tau}_{\text{id}} = 150$ ms, $\bar{\tau}_{\text{ac}} = 75$ ms, $n_0 = 40$, $\xi = 0.85$, $n_0 = 40$, $\zeta = \{0.2, 0.7\}$, and FDTx with $P_{\text{dat}} = P_{\text{max}}$ dB. For fair comparison, we first obtain the optimal configuration of the single-stage FD MAC protocol, i.e., then we use (T^*, p^*) for the HD MAC protocol and FDC-MAC protocol. For the single-stage FD MAC protocol, the transmit power is set to P_{max} because there is only a single stage where the SU performs sensing and transmission simultaneously during the data phase. In addition, the HD MAC protocol will also transmit with the maximum transmit power P_{max} to achieve the highest throughput. For both studied cases of $\zeta = \{0.2, 0.7\}$, our proposed FDC-MAC protocol significantly outperforms the other two protocols. Moreover, the single-stage FD MAC protocol [33] with power allocation outperforms the HD MAC protocol at the corresponding optimal value of P_{max} required by the single-stage FD MAC protocol. However, both single-stage FDC-MAC and HD MAC protocols achieve increasing throughput with higher P_{max} while the single-stage FD MAC protocol has the throughput first increased then decreased as P_{max} increases. This demonstrates the negative self-interference effect on the throughput performance of the single-stage FD MAC protocol, which is efficiently mitigated by our proposed FDC-MAC protocol.

VI. CONCLUSION

In this paper, we have proposed the FDC–MAC protocol for cognitive radio networks, analyzed its throughput performance, and studied its optimal parameter configuration.

The design and analysis have taken into account the FD communication capability and the self-interference of the FD transceiver. We have shown that there exists an optimal FD sensing time to achieve the maximum throughput. We have then presented extensive numerical results to demonstrate the impacts of self-interference and protocol parameters on the throughput performance. In particular, we have shown that the FDC–MAC protocol achieves significantly higher throughput than the HD MAC protocol, which confirms that the FDC–MAC protocol can efficiently exploit the FD communication capability. Moreover, the FDC–MAC protocol results in higher throughput with the increasing maximum power budget while the throughput of the single-stage FD MAC can decrease in the high power regime. This result validates the importance of adopting the two-stage procedure in the data phase and the optimization of sensing time and transmit power during the FD sensing stage to mitigate the negative self-interference effect.

APPENDIX A
DERIVATION OF $\overline{T}_{\text{cont}}$

To calculate $\overline{T}_{\text{cont}}$, we define some further parameters as follows. Denote T_{coll} as the duration of the collision and T_{succ} as the required time for successful RTS/CTS transmission. These quantities can be calculated as follows [17]:

$$\begin{cases} T_{\text{succ}} = DIFS + RTS + SIFS + CTS + 2PD \\ T_{\text{coll}} = DIFS + RTS + PD, \end{cases} \tag{8}$$

where $DIFS$ is the length of a DCF (distributed coordination function) interframe space, RTS and CTS denote the lengths of the RTS and CTS messages, respectively.

As being shown in Fig. 1, there can be several idle periods and collisions before one successful channel reservation. Let T^i_{idle} denote the i-th idle duration between two consecutive RTS/CTS exchanges, which can be collisions or successful exchanges. Then, T^i_{idle} can be calculated based on its probability mass function (pmf), which is derived as follows. In the following, all relevant quantities are defined in terms of the number of time slots. With n_0 SUs joining the contention resolution, let $\mathcal{P}_{\text{succ}}$, $\mathcal{P}_{\text{coll}}$ and $\mathcal{P}_{\text{idle}}$ denote the probabilities that a particular generic slot corresponds to a successful transmission, a collision, and an idle slot, respectively. These probabilities can be calculated as follows:

$$\mathcal{P}_{\text{succ}} = n_0 p\,(1-p)^{n_0-1} \tag{9}$$

$$\mathcal{P}_{\text{idle}} = (1-p)^{n_0} \tag{10}$$

$$\mathcal{P}_{\text{coll}} = 1 - \mathcal{P}_{\text{succ}} - \mathcal{P}_{\text{idle}}, \tag{11}$$

where p is the transmission probability of an SU in a generic slot. In general, the interval T_{cont}, whose average value is $\overline{T}_{\text{cont}}$ given in (2), consists of several intervals corresponding to idle periods, collisions, and one successful RTS/CTS transmission. Hence, this quantity can be expressed as

$$T_{\text{cont}} = \sum_{i=1}^{N_{\text{coll}}} \left(T_{\text{coll}} + T^i_{\text{idle}}\right) + T^{N_{\text{coll}}+1}_{\text{idle}} + T_{\text{succ}}, \tag{12}$$

where N_{coll} is the number of collisions before the successful RTS/CTS exchange and N_{coll} is a geometric random variable (RV) with parameter $1 - \mathcal{P}_{\text{coll}}/\overline{\mathcal{P}}_{\text{idle}}$ where $\overline{\mathcal{P}}_{\text{idle}} = 1 - \mathcal{P}_{\text{idle}}$. Therefore, its pmf can be expressed as

$$f_X^{N_{\text{coll}}}(x) = \left(\frac{\mathcal{P}_{\text{coll}}}{\overline{\mathcal{P}}_{\text{idle}}}\right)^x \left(1 - \frac{\mathcal{P}_{\text{coll}}}{\overline{\mathcal{P}}_{\text{idle}}}\right), \quad x = 0, 1, 2, \ldots \tag{13}$$

Also, T_{idle} represents the number of consecutive idle slots, which is also a geometric RV with parameter $1 - \mathcal{P}_{\text{idle}}$ with the following pmf

$$f_X^{T_{\text{idle}}}(x) = (\mathcal{P}_{\text{idle}})^x (1 - \mathcal{P}_{\text{idle}}), \quad x = 0, 1, 2, \ldots \tag{14}$$

Therefore, $\overline{T}_{\text{cont}}$ (the average value of T_{cont}) can be written as follows [17]:

$$\overline{T}_{\text{cont}} = \overline{N}_{\text{coll}} T_{\text{coll}} + \overline{T}_{\text{idle}} \left(\overline{N}_{\text{coll}} + 1\right) + T_{\text{succ}}, \tag{15}$$

where $\overline{T}_{\text{idle}}$ and $\overline{N}_{\text{coll}}$ can be calculated as

$$\overline{T}_{\text{idle}} = \frac{(1-p)^{n_0}}{1-(1-p)^{n_0}} \tag{16}$$

$$\overline{N}_{\text{coll}} = \frac{1-(1-p)^{n_0}}{n_0 p\,(1-p)^{n_0-1}} - 1. \tag{17}$$

These expressions are obtained by using the pmfs of the corresponding RVs given in (13) and (14), respectively [17].

APPENDIX B
DERIVATIONS OF $\mathcal{B}_1$, $\mathcal{B}_2$, $\mathcal{B}_3$

We will employ a pair of parameters (θ, φ) to represent the HDTX and FDTX modes where $((\theta, \varphi) = (0, 1))$ for HDTx mode and $((\theta, \varphi) = (1, 2))$ for the FDTx mode. Moreover, since the transmit powers in the FD sensing and transmission stages are different, which are equal to P_{sen} and P_{dat}, respectively, we define different SNRs and SINRs in these two stages as follows: $\gamma_{S1} = \frac{P_{\text{sen}}}{N_0}$ and $\gamma_{S2} = \frac{P_{\text{sen}}}{N_0+P_p}$ are the SNR and SINR achieved by the SU in the FD sensing stage with and without the presence of the PU, respectively; $\gamma_{D1} = \frac{P_{\text{dat}}}{N_0+\theta I}$ and $\gamma_{D2} = \frac{P_{\text{dat}}}{N_0+P_p+\theta I}$ for $I = \zeta P^{\xi}_{\text{dat}}$ are the SNR and SINR achieved by the SU in the transmission stage with and without the presence of the PU, respectively. It can be seen that we have accounted for the self-interference for the FDTx mode during the transmission stage in γ_{D1} by noting that $\theta = 1$ in this case. The parameter φ for the HDTx and FDTx modes will be employed to capture the throughput for one-way and two-way transmissions in these modes, respectively.

The derivations of $\mathcal{B}_1$, $\mathcal{B}_2$, and $\mathcal{B}_3$ require us to consider different possible sensing outcomes in the FD sensing stage. In particular, we need to determine the detection probability $\mathcal{P}^{ij}_d$, which is the probability of correctly detecting the PU given the PU is active, and the false alarm probability $\mathcal{P}^{ij}_f$, which is the probability of the erroneous sensing of an idle channel, for each event h_{ij} capturing the state changes of the PU. In the following analysis, we assume the exponential distribution for τ_{ac} and τ_{id} where $\bar{\tau}_{\text{ac}}$ and $\bar{\tau}_{\text{id}}$

denote the corresponding average values of these active and idle intervals. Specifically, let $f_{\tau_{\mathsf{x}}}(t)$ denote the pdf of τ_{x} (x represents ac or id in the pdf of τ_{ac} or τ_{id}, respectively) then

$$f_{\tau_{\mathsf{x}}}(t) = \frac{1}{\bar{\tau}_{\mathsf{x}}} \exp(-\frac{t}{\bar{\tau}_{\mathsf{x}}}). \tag{18}$$

Similarly, we employ T_S^{ij} and T_D^{ij} to denote the number of bits transmitted on one unit of system bandwidth during the FD sensing and transmission stages under the PU's state-changing event h_{ij}, respectively.

We can now calculate $\mathcal{B}_1$ as follows:

$$\begin{aligned}\mathcal{B}_1 &= \mathcal{P}(\mathcal{H}_0) \int_{t=T_{\mathsf{ove}}+T}^{\infty} T_1^{00} f_{\tau_{\mathsf{id}}}(t) dt \\ &= \mathcal{P}(\mathcal{H}_0) T_1^{00} \exp\left(-\frac{T_{\mathsf{ove}}+T}{\bar{\tau}_{\mathsf{id}}}\right),\end{aligned} \tag{19}$$

where $\mathcal{P}(\mathcal{H}_0)$ denotes the probability of the idle state of the PU, and $\mathcal{P}_f^{00}$ is the false alarm probability for event h_{00} given in Appendix C. Moreover, $T_1^{00} = \mathcal{P}_f^{00} T_S^{00} + (1-\mathcal{P}_f^{00})(T_S^{00} + T_D^{00})$, $T_S^{00} = T_S \log_2(1+\gamma_{S1})$, $T_D^{00} = \varphi(T-T_S)\log_2(1+\gamma_{D1})$ where T_S^{00} and T_D^{00} denote the number of bits transmitted (over one Hz of system bandwidth) in the FD sensing and transmission stages of the data phase, respectively. After some manipulations, we achieve

$$\begin{aligned}\mathcal{B}_1 = \mathcal{K}_e \exp\left(\frac{T}{\Delta\tau}\right)\Big[T_S \log_2(1+\gamma_{S1}) + \varphi\left(1-\mathcal{P}_f^{00}\right) \\ \times (T-T_S)\log_2(1+\gamma_{D1})\Big],\end{aligned} \tag{20}$$

where $\mathcal{K}_e = \mathcal{P}(\mathcal{H}_0)\exp\left(-\left(\frac{T_{\mathsf{ove}}}{\bar{\tau}_{\mathsf{id}}} + \frac{T}{\bar{\tau}_{\mathsf{ac}}}\right)\right)$ and $\frac{1}{\Delta\tau} = \frac{1}{\bar{\tau}_{\mathsf{ac}}} - \frac{1}{\bar{\tau}_{\mathsf{id}}}$.

Moreover, we can calculate $\mathcal{B}_2$ as

$$\begin{aligned}\mathcal{B}_2 = \mathcal{P}(\mathcal{H}_0) \int_{t_1=T_{\mathsf{ove}}+T_S}^{T_{\mathsf{ove}}+T} \int_{t_2=T_{\mathsf{ove}}+T-t_1}^{\infty} \\ T_2^{01}(t_1) f_{\tau_{\mathsf{id}}}(t_1) f_{\tau_{\mathsf{ac}}}(t_2) dt_1 dt_2,\end{aligned} \tag{21}$$

where $T_2^{01}(t_1) = \mathcal{P}_f^{00} T_S^{00} + (1-\mathcal{P}_f^{00})(T_S^{00} + T_D^{01}(\bar{t}_1))$, $T_D^{01}(t_1) = \varphi(T-T_S-\bar{t}_1)\log_2(1+\gamma_{D2}) + \varphi\bar{t}_1\log_2(1+\gamma_{D1})$, and $\bar{t}_1 = t_1 - (T_{\mathsf{ove}}+T_S)$. In this expression, t_1 denotes the interval from the beginning of the CA cycle to the instant when the PU changes to the active state from an idle state. Again, T_S^{00} and T_D^{01} denote the amount of data transmitted in the FD sensing and transmission stages for this case, respectively. After some manipulations, we achieve

$$\begin{aligned}\mathcal{B}_2 = \mathcal{K}_e \frac{\Delta\tau}{\bar{\tau}_{\mathsf{id}}} \Bigg\{\left(\exp\left(\frac{T}{\Delta\tau}\right) - \exp\left(\frac{T_S}{\Delta\tau}\right)\right) \\ \times\left[T_S \log_2(1+\gamma_{S1}) - \varphi\Delta\tau\left(1-\mathcal{P}_f^{00}\right)\log_2\left(\frac{1+\gamma_{D1}}{1+\gamma_{D2}}\right)\right] \\ + \varphi(T-T_S)\left(1-\mathcal{P}_f^{00}\right) \\ \times\left[\exp\left(\frac{T}{\Delta\tau}\right)\log_2(1+\gamma_{D1}) - \exp\left(\frac{T_S}{\Delta\tau}\right)\log_2(1+\gamma_{D2})\right]\Bigg\}.\end{aligned} \tag{22}$$

Finally, we can express $\mathcal{B}_3$ as follows:

$$\begin{aligned}\mathcal{B}_3 = \mathcal{P}(\mathcal{H}_0) \int_{t_1=T_{\mathsf{ove}}}^{T_{\mathsf{ove}}+T_S} \int_{t_2=T_{\mathsf{ove}}+T-t_1}^{\infty} \\ \left[\mathcal{P}_d^{01}(\bar{t}_1) T_S^{01}(\bar{t}_1) + (1-\mathcal{P}_d^{01}(\bar{t}_1))(T_S^{01}(\bar{t}_1) + T_D^{11})\right] \\ \times f_{\tau_{\mathsf{id}}}(t_1) f_{\tau_{\mathsf{ac}}}(t_2) dt_1 dt_2,\end{aligned} \tag{23}$$

where $\bar{t}_1 = t_1 - T_{\mathsf{ove}}$, $T_S^{01}(\bar{t}_1) = \bar{t}_1 \log_2(1+\gamma_{S1}) + (T_S - \bar{t}_1)\log_2(1+\gamma_{S2})$, $T_D^{11} = \varphi(T-T_S)\log_2(1+\gamma_{D2})$, and t_1 is the same as in (21). Here, T_S^{01} and T_D^{11} denote the amount of data delivered in the FD sensing and transmission stages for the underlying case, respectively. After some manipulations, we attain

$$\begin{aligned}\mathcal{B}_3 = \mathcal{K}_e \int_{t=0}^{T_S} \left[T_S^{01}(t) + T_D^{11} - \mathcal{P}_d^{01}(t) T_D^{11}\right] \\ \times f_{\tau_{\mathsf{id}}}(t) \exp\left(\frac{t}{\bar{\tau}_{\mathsf{ac}}}\right) dt = \mathcal{B}_{31} + \mathcal{B}_{32},\end{aligned} \tag{24}$$

where

$$\begin{aligned}\mathcal{B}_{31} &= \mathcal{K}_e \int_{t=0}^{T_S} \left[T_S^{01}(t) + T_D^{11}\right] f_{\tau_{\mathsf{id}}}(t) \exp\left(\frac{t}{\bar{\tau}_{\mathsf{ac}}}\right) dt \\ &= \mathcal{K}_e \frac{\Delta\tau}{\bar{\tau}_{\mathsf{id}}} \Bigg\{\Delta\tau\left[\left(\frac{T_S}{\Delta\tau}-1\right)\exp\left(\frac{T_S}{\Delta\tau}\right)+1\right]\log_2\left(\frac{1+\gamma_{S1}}{1+\gamma_{S2}}\right) \\ &\quad + \left[\exp\left(\frac{T_S}{\Delta\tau}\right)-1\right]\left[T_D^{11} + T_S\log_2(1+\gamma_{S2})\right]\Bigg\},\end{aligned} \tag{25}$$

and

$$\mathcal{B}_{32} = -\mathcal{K}_e T_D^{11} \bar{T}_{32}, \tag{26}$$

where $\bar{T}_{32} = \int_{t=0}^{T_S} \mathcal{P}_d^{01}(t) f_{\tau_{\mathsf{id}}}(t) \exp\left(\frac{t}{\bar{\tau}_{\mathsf{ac}}}\right) dt$.

APPENDIX C
FALSE ALARM AND DETECTION PROBABILITIES

We derive the detection and false alarm probabilities for FD sensing and two PU's state-changing events h_{00} and h_{01} in this appendix. Assume that the transmitted signals from the PU and SU are circularly symmetric complex Gaussian (CSCG) signals while the noise at the secondary receiver is independently and identically distributed CSCG $\mathcal{CN}(0, N_0)$ [5]. Under FD sensing, the false alarm probability for event h_{00} can be derived using the similar method as in [5], which is given as

$$\mathcal{P}_f^{00} = \mathcal{Q}\left[\left(\frac{\epsilon}{N_0 + I(P_{\mathsf{sen}})} - 1\right)\sqrt{f_s T_S}\right], \tag{27}$$

where $\mathcal{Q}(x) = \int_x^{+\infty} \exp\left(-t^2/2\right) dt$; $f_s, N_0, \epsilon, I(P_{\mathsf{sen}})$ are the sampling frequency, the noise power, the detection threshold and the self-interference, respectively; T_S is the FD sensing duration.

The detection probability for event h_{01} is given as

$$\mathcal{P}_d^{01} = \mathcal{Q}\left(\frac{\left(\frac{\epsilon}{N_0+I(P_{\mathsf{sen}})} - \frac{T_S-t}{T_S}\gamma_{PS} - 1\right)\sqrt{f_s T_S}}{\sqrt{\frac{T_S-t}{T_S}(\gamma_{PS}+1)^2 + \frac{t}{T_S}}}\right), \tag{28}$$

where t is the interval from the beginning of the data phase to the instant when the PU changes its state, $\gamma_{PS} = \frac{P_p}{N_0 + I(P_{\text{sen}})}$ is the signal-to-interference-plus-noise ratio (SINR) of the PU's signal at the SU.

APPENDIX D
PROOF OF THEOREM 1

The first derivative of $\mathcal{NT}$ can be written as follows:

$$\frac{\partial \mathcal{NT}}{\partial T_S} = \frac{1}{T_{\text{ove}} + T} \sum_{i=1}^{3} \frac{\partial \mathcal{B}_i}{\partial T_S}. \tag{29}$$

We derive the first derivative of $\mathcal{B}_i$ $(i = 1, 2, 3)$ in the following. Toward this end, we will employ the approximation of $\exp(x) \approx 1 + x$, $x = \frac{T_x}{\tau_x}$, $T_x \in \{T, T_S, T - T_S\}$, $\tau_x \in \{\bar{\tau}_{\text{id}}, \bar{\tau}_{\text{ac}}, \Delta\tau\}$ where recall that $\frac{1}{\Delta\tau} = \frac{1}{\bar{\tau}_{\text{ac}}} - \frac{1}{\bar{\tau}_{\text{id}}}$. This approximation holds under the assumption that $T_x << \tau_x$ since we can omit all higher-power terms x^n for $n > 1$ from the Maclaurin series expansion of function $\exp(x)$. Using this approximation, we can express the first derivative of $\mathcal{B}_1$ as

$$\frac{\partial \mathcal{B}_1}{\partial T_S} = \mathcal{K}_e \exp\left(\frac{T}{\Delta\tau}\right) \Bigg\{ \log_2(1 + \gamma_{S1}) - \varphi \left[(T - T_S) \frac{\partial \mathcal{P}_f^{00}}{\partial T_S} + \left(1 - \mathcal{P}_f^{00}\right) \right] \log_2(1 + \gamma_{D1}) \Bigg\}, \tag{30}$$

where $\frac{\partial \mathcal{P}_f^{00}}{\partial T_S}$ is the first derivative of $\mathcal{P}_f^{00}$ whose derivation is given in Appendix E.

Moreover, the first derivative of $\mathcal{B}_2$ can be written as

$$\begin{aligned}
\frac{\partial \mathcal{B}_2}{\partial T_S} &= \mathcal{K}_e \frac{\Delta\tau}{\bar{\tau}_{\text{id}}} \\
&\times \Bigg\{ \left[\exp\left(\frac{T}{\Delta\tau}\right) - \left(1 + \frac{T}{\Delta\tau}\right) \exp\left(\frac{T_S}{\Delta\tau}\right) \right] \log_2(1 + \gamma_{S1}) \\
&- \varphi \frac{\partial \mathcal{P}_f^{00}}{\partial T_S} \Bigg[\Delta\tau \left(\exp\left(\frac{T_S}{\Delta\tau}\right) - \exp\left(\frac{T}{\Delta\tau}\right) \right) \log_2\left(\frac{1+\gamma_{D1}}{1+\gamma_{D2}}\right) \\
&+ (T - T_S) \left(\exp\left(\frac{T}{\Delta\tau}\right) \log_2(1+\gamma_{D1}) - \exp\left(\frac{T_S}{\Delta\tau}\right) \log_2(1+\gamma_{D2}) \right) \Bigg] \\
&+ \varphi \left(1 - \mathcal{P}_f^{00}\right) \Bigg[-\frac{T - T_S}{\Delta\tau} \exp\left(\frac{T_S}{\Delta\tau}\right) \log_2(1 + \gamma_{D2}) \\
&- \left(\exp\left(\frac{T}{\Delta\tau}\right) \log_2(1+\gamma_{D1}) - \exp\left(\frac{T_S}{\Delta\tau}\right) \log_2(1+\gamma_{D2}) \right) \\
&+ \exp\left(\frac{T_S}{\Delta\tau}\right) \log_2\left(\frac{1+\gamma_{D1}}{1+\gamma_{D2}}\right) \Bigg] \Bigg\}.
\end{aligned} \tag{31}$$

Finally, the first derivative of $\mathcal{B}_3$ can be written as

$$\frac{\partial \mathcal{B}_3}{\partial T_S} = \frac{\partial \mathcal{B}_{31}}{\partial T_S} + \frac{\partial \mathcal{B}_{32}}{\partial T_S}, \tag{32}$$

where

$$\begin{aligned}
\frac{\partial \mathcal{B}_{31}}{\partial T_S} &= \mathcal{K}_e \frac{\Delta\tau}{\bar{\tau}_{\text{id}}} \Bigg\{ \Delta\tau \left[1 + \left(\frac{T_S}{\Delta\tau} - 1 \right) \exp\left(\frac{T_S}{\Delta\tau}\right) \right] \\
&\times \log_2\left(\frac{1+\gamma_{S1}}{1+\gamma_{S2}}\right) + \left(\exp\left(\frac{T_S}{\Delta\tau}\right) - 1 \right) \\
&\times \left[T_S \log_2(1+\gamma_{S2}) + \varphi(T - T_S) \log_2(1+\gamma_{D2}) \right] \Bigg\}.
\end{aligned} \tag{33}$$

To obtain the derivative for $\mathcal{B}_{32}$, we note that $1 \leq \exp\left(\frac{t}{\bar{\tau}_{\text{ac}}}\right) \leq \exp\left(\frac{T_S}{\bar{\tau}_{\text{ac}}}\right)$ for $\forall t \in [0, T_S]$. Moreover, from the results in (5) and (6) and using the definition of $\bar{T}_{32}$ in (26), we have $\overline{\mathcal{P}}_d \left(1 - \exp\left(\frac{-T_S}{\bar{\tau}_{\text{id}}}\right)\right) \leq \bar{T}_{32} \leq \overline{\mathcal{P}}_d \left(1 - \exp\left(\frac{-T_S}{\bar{\tau}_{\text{id}}}\right)\right) \exp\left(\frac{T_S}{\bar{\tau}_{\text{ac}}}\right)$. Using these results, the first derivative of $\mathcal{B}_{32}$ can be expressed as

$$\frac{\partial \mathcal{B}_{32}}{\partial T_S} = -\mathcal{K}_e \overline{\mathcal{P}}_d \varphi \frac{T - 2T_S}{\bar{\tau}_{\text{id}}} \log_2(1 + \gamma_{D2}). \tag{34}$$

Therefore, we have obtained the first derivative of $\mathcal{NT}$ and we are ready to prove the first statement of Theorem 1. Substitute $T_S = 0$ to the derived $\frac{\partial \mathcal{NT}}{\partial T_S}$ and use the approximation $\exp(x) \approx 1 + x$, we yield the following result after some manipulations

$$\lim_{T_S \to 0} \frac{\partial \mathcal{NT}}{\partial T_S} = -K_0 K_1 \lim_{T_S \to 0} \frac{\partial \mathcal{P}_f^{00}}{\partial T_S}, \tag{35}$$

where $K_0 = \frac{1}{T_{\text{ove}} + T} \mathcal{K}_e$ and

$$\begin{aligned}
K_1 &= \varphi \left[T \left(1 + \frac{T}{\Delta\tau} \right) + \frac{T^2}{\bar{\tau}_{\text{id}}} \right] \log_2(1 + \gamma_{D1}) \\
&+ \varphi \frac{T \Delta\tau}{\bar{\tau}_{\text{id}}} \log_2(1 + \gamma_{D2}).
\end{aligned} \tag{36}$$

It can be verified that $K_0 > 0$, $K_1 > 0$ and $\lim_{T_S \to 0} \frac{\partial \mathcal{P}_f^{00}}{\partial T_S} = -\infty$ by using the derivations in Appendix E; hence, we have $\lim_{T_S \to 0} \frac{\partial \mathcal{NT}}{\partial T_S} = +\infty > 0$. This completes the proof of the first statement of the theorem.

We now present the proof for the second statement of the theorem. Substitute $T_S = T$ to $\frac{\partial \mathcal{NT}}{\partial T_S}$ and utilize the approximation $\exp(x) \approx 1 + x$, we yield

$$\lim_{T_S \to T} \frac{\partial \mathcal{NT}}{\partial T_S} = \frac{1}{T_{\text{ove}} + T} \sum_{i=1}^{3} \frac{\partial \mathcal{B}_i}{\partial T_S}(T), \tag{37}$$

where we have

$$\begin{aligned}
\frac{\partial \mathcal{B}_1}{\partial T_S}(T) &= \mathcal{K}_e \left(1 + \frac{T}{\Delta\tau}\right) \\
&\times \left[\log_2(1 + \gamma_{S1}) - \varphi \left(1 - \mathcal{P}_f^{00}(T)\right) \log_2(1 + \gamma_{D1}) \right]
\end{aligned} \tag{38}$$

$$\frac{\partial \mathcal{B}_2}{\partial T_S}(T) = -\mathcal{K}_e \frac{T}{\bar{\tau}_{\text{id}}} \log_2(1 + \gamma_{S1}) \tag{39}$$

$$\frac{\partial \mathcal{B}_{31}}{\partial T_S}(T) = \mathcal{K}_e \frac{T}{\bar{\tau}_{\mathsf{id}}}[\log_2(1+\gamma_{S1})(1+\gamma_{S2}) - \varphi \log_2(1+\gamma_{D2})] \tag{40}$$

$$\frac{\partial \mathcal{B}_{32}}{\partial T_S}(T) = \mathcal{K}_e \varphi \frac{T}{\bar{\tau}_{\mathsf{id}}} \overline{\mathcal{P}}_d \log_2(1+\gamma_{D2}).$$

Omit all high-power terms in the expansion of $\exp(x)$ (i.e., x^n with $n > 1$) where $x = \frac{T_x}{\tau_x}$, $T_x \in \{T, T_S, T - T_S\}$, $\tau_x \in \{\bar{\tau}_{\mathsf{id}}, \bar{\tau}_{\mathsf{ac}}, \Delta\tau\}$, we yield

$$\lim_{T_S \to T} \frac{\partial \mathcal{NT}}{\partial T_S} \approx \frac{1}{T_{\mathsf{ove}} + T} \frac{\partial \mathcal{B}_1}{\partial T_S}(T). \tag{41}$$

We consider the HDTx and FDTx modes in the following. For the HDTx mode, we have $\varphi = 1$ and $\theta = 0$. Then, it can be verified that $\lim_{T_S \to T} \frac{\partial \mathcal{NT}}{\partial T_S} < 0$ by using the results in (38) and (41). This is because we have $\log_2(1+\gamma_{S1}) - \left(1 - \mathcal{P}_f^{00}(T)\right)\log_2(1+\gamma_{D1}) \approx \log_2(1+\gamma_{S1}) - \log_2(1+\gamma_{D1}) < 0$ (since we have $\mathcal{P}_f^{00}(T) \approx 0$ and $\gamma_{S1} \le \gamma_{D1}$).

For the FDTx mode, we have $\varphi = 2, \theta = 1$, and also $\gamma_{S1} = \frac{P_{\mathsf{sen}}}{N_0}$ and $\gamma_{D1} = \frac{P_{\mathsf{dat}}}{N_0 + I(P_{\mathsf{dat}})} = \frac{P_{\mathsf{dat}}}{N_0 + \zeta P_{\mathsf{dat}}^{\xi}}$. We would like to define a critical value of P_{sen} which satisfies $\lim_{T_S \to T} \frac{\partial \mathcal{NT}}{\partial T_S} = 0$ to proceed further. Using the result in (38) and (41) as well as the approximation $\mathcal{P}_f^{00}(T) \approx 0$, and by solving $\lim_{T_S \to T} \frac{\partial \mathcal{NT}}{\partial T_S} = 0$ we yield

$$\overline{P}_{\mathsf{sen}} = N_0 \left[\left(1 + \frac{P_{\mathsf{dat}}}{N_0 + \zeta P_{\mathsf{dat}}^{\xi}}\right)^2 - 1 \right]. \tag{42}$$

Using (38), it can be verified that if $P_{\mathsf{sen}} > \overline{P}_{\mathsf{sen}}$ then $\lim_{T_S \to T} \frac{\partial \mathcal{NT}}{\partial T_S} > 0$; otherwise, we have $\lim_{T_S \to T} \frac{\partial \mathcal{NT}}{\partial T_S} \le 0$. So we have completed the proof for the second statement of Theorem 1.

To prove the third statement of the theorem, we derive the second derivative of $\mathcal{NT}$ as

$$\frac{\partial^2 \mathcal{NT}}{\partial T_S^2} = \frac{1}{T_{\mathsf{ove}} + T} \sum_{i=1}^{3} \frac{\partial^2 \mathcal{B}_i}{\partial T_S^2}, \tag{43}$$

where we have

$$\frac{\partial^2 \mathcal{B}_1}{\partial T_S^2} = -\mathcal{K}_e \varphi \exp\left(\frac{T}{\Delta\tau}\right) \log_2(1+\gamma_{D1}) \times \left[(T - T_S) \frac{\partial^2 \mathcal{P}_f^{00}}{\partial T_S^2} - 2 \frac{\partial \mathcal{P}_f^{00}}{\partial T_S} \right], \tag{44}$$

where $\frac{\partial^2 \mathcal{P}_f^{00}}{\partial T_S^2}$ is the second derivative of $\mathcal{P}_f^{00}$ and according to the derivations in Appendix E, we have $\frac{\partial^2 \mathcal{P}_f^{00}}{\partial T_S^2} > 0$, $\frac{\partial \mathcal{P}_f^{00}}{\partial T_S} < 0$, $\forall T_S$. Therefore, we yield $\frac{\partial^2 \mathcal{B}_1}{\partial T_S^2} < 0 \; \forall T_S$.

Consequently, we have the following upper bound for $\frac{\partial^2 \mathcal{B}_1}{\partial T_S^2}$ by omitting the term $\exp\left(\frac{T}{\Delta\tau}\right) > 1$ in (44)

$$\frac{\partial^2 \mathcal{B}_1}{\partial T_S^2} \le \mathcal{K}_e \left[h_1(T_S) + h_2(T_S) \right], \tag{45}$$

where

$$h_1(T_S) = -\varphi (T - T_S) \frac{\partial^2 \mathcal{P}_f^{00}}{\partial T_S^2} \log_2(1+\gamma_{D1}),$$

$$h_2(T_S) = 2\varphi \frac{\partial \mathcal{P}_f^{00}}{\partial T_S} \log_2(1+\gamma_{D1}).$$

Moreover, we have

$$\begin{aligned}
\frac{\partial^2 \mathcal{B}_2}{\partial T_S^2} = \frac{\mathcal{K}_e \Delta\tau}{\bar{\tau}_{\mathsf{id}}} \Bigg\{ & -\frac{2 + \frac{T_S}{\Delta\tau}}{\Delta\tau} \exp\left(\frac{T_S}{\Delta\tau}\right) \log_2(1+\gamma_{S1}) \\
& - \varphi \frac{\partial^2 \mathcal{P}_f^{00}}{\partial T_S^2} \Bigg[\Delta\tau \left(\exp\left(\frac{T_S}{\Delta\tau}\right) - \exp\left(\frac{T}{\Delta\tau}\right) \right) \log_2\left(\frac{1+\gamma_{D1}}{1+\gamma_{D2}}\right) \\
& + (T - T_S) \left(\exp\left(\frac{T}{\Delta\tau}\right) \log_2(1+\gamma_{D1}) \right. \\
& \left. - \exp\left(\frac{T_S}{\Delta\tau}\right) \log_2(1+\gamma_{D2}) \right) \Bigg] \\
& + 2\varphi \frac{\partial \mathcal{P}_f^{00}}{\partial T_S} \Bigg[\left(\exp\left(\frac{T}{\Delta\tau}\right) - \exp\left(\frac{T_S}{\Delta\tau}\right) \right) \log_2(1+\gamma_{D1}) \\
& + \frac{T - T_S}{\Delta\tau} \exp\left(\frac{T_S}{\Delta\tau}\right) \log_2(1+\gamma_{D2}) \Bigg] \\
& - \varphi \left(1 - \mathcal{P}_f^{00}\right) \frac{T - T_S}{\Delta\tau} \exp\left(\frac{T_S}{\Delta\tau}\right) \log_2(1+\gamma_{D2}) \\
& + \varphi \left(1 - \mathcal{P}_f^{00}\right) \frac{1}{\Delta\tau} \exp\left(\frac{T_S}{\Delta\tau}\right) \log_2\left(\frac{1+\gamma_{D1}}{1+\gamma_{D2}}\right) \Bigg\}.
\end{aligned} \tag{46}$$

Therefore, we can approximate $\frac{\partial^2 \mathcal{B}_2}{\partial T_S^2}$ as follows:

$$\frac{\partial^2 \mathcal{B}_2}{\partial T_S^2} = \mathcal{K}_e \left[h_3(T_S) + h_4(T_S) + h_5(T_S) \right], \tag{47}$$

where

$$h_3(T_S) = -\frac{\left(2 + \frac{T_S}{\Delta\tau}\right)\left(1 + \frac{T_S}{\Delta\tau}\right)}{\bar{\tau}_{\mathsf{id}}} \log_2(1+\gamma_{S1}),$$

$$\begin{aligned}
h_4(T_S) = & -\varphi \left(1 - \mathcal{P}_f^{00}\right) \frac{T - T_S}{\bar{\tau}_{\mathsf{id}}} \left(1 + \frac{T_S}{\Delta\tau}\right) \log_2(1+\gamma_{D2}) \\
& - \varphi \frac{\partial^2 \mathcal{P}_f^{00}}{\partial T_S^2} (T - T_S) \left[\frac{T}{\bar{\tau}_{\mathsf{id}}} \log_2(1+\gamma_{D1}) - \frac{T_S}{\bar{\tau}_{\mathsf{id}}} \log_2(1+\gamma_{D2}) \right] \\
& + 2\varphi \frac{\partial \mathcal{P}_f^{00}}{\partial T_S} \frac{T - T_S}{\bar{\tau}_{\mathsf{id}}} \left[\log_2\left(\frac{1+\gamma_{D1}}{1+\gamma_{D2}}\right) + \frac{T_S}{\Delta\tau} \log_2(1+\gamma_{D2}) \right],
\end{aligned}$$

$$h_5(T_S) = \varphi \left(1 - \mathcal{P}_f^{00}\right) \frac{1}{\bar{\tau}_{\mathsf{id}}} \left(1 + \frac{T_S}{\Delta\tau}\right) \log_2\left(\frac{1+\gamma_{D1}}{1+\gamma_{D2}}\right).$$

In addition, we have

$$\begin{aligned}
\frac{\partial^2 \mathcal{B}_{31}}{\partial T_S^2} = \frac{\mathcal{K}_e}{\bar{\tau}_{\mathsf{id}}} \exp\left(\frac{T_S}{\Delta\tau}\right) \Bigg\{ & \left(1 + \frac{T}{\Delta\tau}\right) \log_2(1+\gamma_{S1}) \\
& + \log_2(1+\gamma_{S2}) + \varphi \left(\frac{T - T_S}{\Delta\tau} - 2 \right) \log_2(1+\gamma_{D2}) \Bigg\}.
\end{aligned} \tag{48}$$

We can approximate $\frac{\partial^2 \mathcal{B}_{31}}{\partial T_S^2}$ as follows:

$$\frac{\partial^2 \mathcal{B}_{31}}{\partial T_S^2} = \mathcal{K}_e \left[h_6(T_S) + h_6(T_S)\right], \tag{49}$$

where

$$h_6(T_S) = \frac{1}{\bar{\tau}_{\text{id}}} \log_2 (1+\gamma_{S1})(1+\gamma_{S2}),$$
$$h_7(T_S) = -\frac{2\varphi}{\bar{\tau}_{\text{id}}} \log_2 (1+\gamma_{D2}). \tag{50}$$

Finally, we have

$$\frac{\partial^2 \mathcal{B}_{32}}{\partial T_S^2} = \mathcal{K}_e h_8(T_S), \tag{51}$$

where

$$h_8(T_S) = \frac{2\varphi \bar{\mathcal{P}}_d}{\bar{\tau}_{\text{id}}} \log_2 (1+\gamma_{D2}). \tag{52}$$

The above analysis yields $\frac{\partial^2 \mathcal{NT}}{\partial T_S^2} = \mathcal{K}_e \sum_{i=1}^{8} h_i(T_S)$. Therefore, to prove that $\frac{\partial^2 \mathcal{NT}}{\partial T_S^2} < 0$, we should prove that $h(T_S) < 0$ since $\mathcal{K}_e > 0$ where

$$h(T_S) = \sum_{i=1}^{8} h_i(T_S). \tag{53}$$

It can be verified that $h_1(T_S) < 0$ and $h_4(T_S) < 0$, $\forall T_S$ because $\frac{\partial^2 \mathcal{P}_f^{00}}{\partial T_S^2} > 0$, $\frac{\partial \mathcal{P}_f^{00}}{\partial T_S} < 0$ according to Appendix E and $\gamma_{D2} < \gamma_{D1}$. Moreover, we have

$$h_3(T_S) < -\frac{2}{\bar{\tau}_{\text{id}}} \log_2 (1+\gamma_{S1}), \tag{54}$$

and because $\gamma_{S1} > \gamma_{S2}$, we have

$$h_3(T_S) < -\frac{1}{\bar{\tau}_{\text{id}}} \log_2 (1+\gamma_{S1})(1+\gamma_{S2}) = -h_6(T_S). \tag{55}$$

Therefore, we have $h_3(T_S)+h_6(T_S) < 0$. Furthermore, we can also obtain the following result $h_7(T_S) + h_8(T_S) \leq 0$ because $\bar{\mathcal{P}}_d \leq 1$. To complete the proof, we must prove that $h_2(T_S) + h_5(T_S) \leq 0$, which is equivalent to

$$-2\bar{\tau}_{\text{id}} \frac{\partial \mathcal{P}_f^{00}}{\partial T_S} \frac{\log_2 (1+\gamma_{D1})}{\log_2 \left(\frac{1+\gamma_{D1}}{1+\gamma_{D2}}\right)} \geq \left(1 - \mathcal{P}_f^{00}\right)\left(1 + \frac{T_S}{\Delta\tau}\right), \tag{56}$$

where according to Appendix E

$$\frac{\partial \mathcal{P}_f^{00}}{\partial T_S} = -\frac{\bar{\gamma}\sqrt{f_s T_S}}{2\sqrt{2\pi} T_S} \exp\left(-\frac{\left(\bar{\alpha} + \bar{\gamma}\sqrt{f_s T_S}\right)^2}{2}\right), \tag{57}$$

where $\bar{\alpha} = (\bar{\gamma}_1 + 1)\, \mathcal{Q}^{-1}\left(\overline{\mathcal{P}}_d\right)$. It can be verified that (56) indeed holds because the LHS of (56) is always larger than to 2 while the RHS of (56) is always less than 2. Hence, we have completed the proof of the third statement of Theorem 1.

Finally, the fourth statement in the theorem obviously holds because $\mathcal{B}_i$ $(i = 1, 2, 3)$ are all bounded from above. Hence, we have completed the proof of Theorem 1.

APPENDIX E
APPROXIMATION OF $\mathcal{P}_f^{00}$ AND ITS FIRST AND SECOND DERIVATIVES

We can approximate $\hat{\mathcal{P}}_d$ in (5) as follows:

$$\hat{\mathcal{P}}_d = \mathcal{Q}\left[\left(\frac{\epsilon}{N_0 + I} - \bar{\gamma} - 1\right)\frac{\sqrt{f_s T_S}}{\bar{\gamma}_1 + 1}\right], \tag{58}$$

where $\bar{\gamma}$ and $\bar{\gamma}_1$ are evaluated by a numerical method. Hence, $\mathcal{P}_f^{00}$ can be calculated as we set $\hat{\mathcal{P}}_d = \overline{\mathcal{P}}_d$, which is given as follows:

$$\mathcal{P}_f^{00} = \mathcal{Q}\left(\bar{\alpha} + \bar{\gamma}\sqrt{f_s T_S}\right), \tag{59}$$

where $\bar{\alpha} = (\bar{\gamma}_1 + 1)\, \mathcal{Q}^{-1}\left(\overline{\mathcal{P}}_d\right)$.

We now derive the first derivative of $\mathcal{P}_f^{00}$ as

$$\frac{\partial \mathcal{P}_f^{00}}{\partial T_S} = -\frac{\bar{\gamma}\sqrt{f_s T_S}}{2\sqrt{2\pi} T_S} \exp\left(-\frac{\left(\bar{\alpha} + \bar{\gamma}\sqrt{f_s T_S}\right)^2}{2}\right). \tag{60}$$

It can be seen that $\frac{\partial \mathcal{P}_f^{00}}{\partial T_S} < 0$ since $\bar{\gamma} > 0$. Moreover, the second derivative of $\mathcal{P}_f^{00}$ is

$$\frac{\partial^2 \mathcal{P}_f^{00}}{\partial T_S^2} = \frac{\bar{\gamma}\sqrt{f_s T_S}}{4\sqrt{2\pi} T_S^2}\left(1 + \frac{1}{2} y \bar{\gamma}\sqrt{f_s T_S}\right) \exp\left(-\frac{y^2}{2}\right), \tag{61}$$

where $y = \bar{\alpha} + \bar{\gamma}\sqrt{f_s T_S}$.

We can prove that $\frac{\partial^2 \mathcal{P}_f^{00}}{\partial T_S^2} > 0$ by considering two different cases as follows. For the first case with $\frac{\bar{\alpha}^2}{\bar{\gamma}^2 f_s} \leq T_S \leq T$ $(0 \leq \mathcal{P}_f^{00} \leq 0.5)$, this statement holds since $y > 0$. For the second case with $0 \leq T_S \leq \frac{\bar{\alpha}^2}{\bar{\gamma}^2 f_s}$ $(0.5 \leq \mathcal{P}_f^{00} \leq 1)$, $y \leq 0$, then we have $0 < y - \bar{\alpha} = \bar{\gamma}\sqrt{f_s T_S} \leq -\bar{\alpha}$ and $0 \leq -y \leq -\bar{\alpha}$. By applying the Cauchy-Schwarz inequality, we obtain $0 \leq -y(y - \bar{\alpha}) \leq \frac{\bar{\gamma}^2}{4} < 1 < 2$; hence $1 + \frac{1}{2} y \bar{\gamma}\sqrt{f_s T_S} > 0$. This result implies that $\frac{\partial^2 \mathcal{P}_f^{00}}{\partial T_S^2} > 0$.

REFERENCES

[1] C. Cormio and K. R. Chowdhury, "A survey on MAC protocols for cognitive radio networks," *Ad Hoc Netw.*, vol. 7, no. 7, pp. 1315–1329, Sep. 2009.
[2] T. Yucek and H. Arslan, "A survey of spectrum sensing algorithms for cognitive radio applications," *IEEE Commun. Surveys Tuts.*, vol. 11, no. 1, pp. 116–130, First Quarter 2009.
[3] Y.-C. Liang, K.-C. Chen, G. Y. Li, and P. Mahonen, "Cognitive radio networking and communications: An overview," *IEEE Trans. Veh. Technol.*, vol. 60, no. 7, pp. 3386–3407, Sep. 2011.
[4] Y. Zou, Y.-D. Yao, and B. Zheng, "Cooperative relay techniques for cognitive radio systems: Spectrum sensing and secondary user transmissions," *IEEE Commun. Mag.*, vol. 50, no. 4, pp. 98–103, Apr. 2012.
[5] Y.-C. Liang, Y. Zeng, E. C. Y. Peh, and A. T. Hoang, "Sensing-throughput tradeoff for cognitive radio networks," *IEEE Trans. Wireless Commun.*, vol. 7, no. 4, pp. 1326–1337, Apr. 2008.
[6] L. T. Tan and L. B. Le, "Distributed MAC protocol for cognitive radio networks: Design, analysis, and optimization," *IEEE Trans. Veh. Technol.*, vol. 60, no. 8, pp. 3990–4003, Oct. 2011.
[7] L. T. Tan and L. B. Le, "Joint cooperative spectrum sensing and MAC protocol design for multi-channel cognitive radio networks," *EURASIP J. Wireless Commun. Netw.*, vol. 2014, p. 101, Dec. 2014.
[8] L. T. Tan and L. B. Le, "Channel assignment with access contention resolution for cognitive radio networks," *IEEE Trans. Veh. Technol.*, vol. 61, no. 6, pp. 2808–2823, Jul. 2012.

[9] Q. Zhao, L. Tong, A. Swami, and Y. Chen, "Decentralized cognitive MAC for opportunistic spectrum access in ad hoc networks: A POMDP framework," *IEEE J. Sel. Areas Commun.*, vol. 25, no. 3, pp. 589–600, Apr. 2007.

[10] H. Kim and K. G. Shin, "Efficient discovery of spectrum opportunities with MAC-layer sensing in cognitive radio networks," *IEEE Trans. Mobile Comput.*, vol. 7, no. 5, pp. 533–545, May 2008.

[11] F. Wang, M. Krunz, and S. Cui, "Price-based spectrum management in cognitive radio networks," *IEEE J. Sel. Topics Signal Process.*, vol. 2, no. 1, pp. 74–87, Feb. 2008.

[12] S. Haykin, D. J. Thomson, and J. H. Reed, "Spectrum sensing for cognitive radio," *Proc. IEEE*, vol. 97, no. 5, pp. 849–877, May 2009.

[13] E. Axell, G. Leus, E. G. Larsson, and H. V. Poor, "Spectrum sensing for cognitive radio: State-of-the-art and recent advances," *IEEE Signal Process. Mag.*, vol. 29, no. 3, pp. 101–116, May 2012.

[14] Y. R. Kondareddy and P. Agrawal, "Synchronized MAC protocol for multi-hop cognitive radio networks," in *Proc. IEEE ICC*, May 2008, pp. 3198–3202.

[15] C. Thorpe and L. Murphy, "A survey of adaptive carrier sensing mechanisms for IEEE 802.11 wireless networks," *IEEE Commun. Surveys Tuts.*, vol. 16, no. 3, pp. 1266–1293, Third Quarter 2014.

[16] G. Bianchi, "Performance analysis of the IEEE 802.11 distributed coordination function," *IEEE J. Sel. Areas Commun.*, vol. 18, no. 3, pp. 535–547, Mar. 2000.

[17] F. Cali, M. Conti, and E. Gregori, "Dynamic tuning of the IEEE 802.11 protocol to achieve a theoretical throughput limit," *IEEE/ACM Trans. Netw.*, vol. 8, no. 6, pp. 785–799, Dec. 2000.

[18] H. S. Chhaya and S. Gupta, "Performance modeling of asynchronous data transfer methods of IEEE 802.11 MAC protocol," *Wireless Netw.*, vol. 3, no. 3, pp. 217–234, Aug. 1997.

[19] I. F. Akyildiz, J. McNair, L. C. Martorell, R. Puigjaner, and Y. Yesha, "Medium access control protocols for multimedia traffic in wireless networks," *IEEE Netw.*, vol. 13, no. 4, pp. 39–47, Jul./Aug. 1999.

[20] M. Duarte, C. Dick, and A. Sabharwal, "Experiment-driven characterization of full-duplex wireless systems," *IEEE Trans. Wireless Commun.*, vol. 11, no. 12, pp. 4296–4307, Dec. 2012.

[21] E. Everett, A. Sahai, and A. Sabharwal, "Passive self-interference suppression for full-duplex infrastructure nodes," *IEEE Trans. Wireless Commun.*, vol. 13, no. 2, pp. 680–694, Jan. 2014.

[22] A. Sabharwal, P. Schniter, D. Guo, D. W. Bliss, S. Rangarajan, and R. Wichman, "In-band full-duplex wireless: Challenges and opportunities," *IEEE J. Sel. Areas Commun.*, vol. 32, no. 9, pp. 1637–1652, Sep. 2014.

[23] D. Korpi, L. Anttila, V. Syrjala, and M. Valkama, "Widely linear digital self-interference cancellation in direct-conversion full-duplex transceiver," *IEEE J. Sel. Areas Commun.*, vol. 32, no. 9, pp. 1674–1687, Sep. 2014.

[24] J. I. Choi, M. Jain, K. Srinivasan, P. Levis, and S. Katti, "Achieving single channel, full duplex wireless communication," in *Proc. ACM 16th Annu. Int. Conf. MobiCom*, 2010, pp. 1–12.

[25] M. Jain *et al.*, "Practical, real-time, full duplex wireless," in *Proc. ACM 17th Annu. Int. Conf. MobiCom*, 2011, pp. 301–312.

[26] E. Hossain, L. B. Le, and D. Niyato, *Radio Resource Management in Multi-Tier Cellular Wireless Networks*. New York, NY, USA: Wiley, 2013.

[27] L. B. Le *et al.*, "Enabling 5G mobile wireless technologies," *EURASIP J. Wireless Commun. Netw.*, vol. 2015, p. 218, Dec. 2015.

[28] M. Duarte *et al.*, "Design and characterization of a full-duplex multi-antenna system for WiFi networks," *IEEE Trans. Veh. Technol.*, vol. 63, no. 3, pp. 1160–1177, Mar. 2014.

[29] S. Goyal, P. Liu, O. Gurbuz, E. Erkip, and S. Panwar, "A distributed MAC protocol for full duplex radio," in *Proc. Asilomar Conf. Signals, Syst., Comput.*, Nov. 2013, pp. 788–792.

[30] D. Ramirez and B. Aazhang, "Optimal routing and power allocation for wireless networks with imperfect full-duplex nodes," *IEEE Trans. Wireless Commun.*, vol. 12, no. 9, pp. 4692–4704, Sep. 2013.

[31] W. Choi, H. Lim, and A. Sabharwal, "Power-controlled medium access control protocol for full-duplex WiFi networks," *IEEE Trans. Wireless Commun.*, vol. 14, no. 7, pp. 3601–3613, Jul. 2015.

[32] W. Cheng, X. Zhang, and H. Zhang, "Full-duplex spectrum-sensing and MAC-protocol for multichannel nontime-slotted cognitive radio networks," *IEEE J. Sel. Areas Commun.*, vol. 33, no. 5, pp. 820–831, May 2015.

[33] L. T. Tan and L. B. Le, "Distributed MAC protocol design for full-duplex cognitive radio networks," in *Proc. IEEE GLOBECOM*, To Appear.

[34] H. Kim, S. Lim, H. Wang, and D. Hong, "Optimal power allocation and outage analysis for cognitive full duplex relay systems," *IEEE Trans. Wireless Commun.*, vol. 11, no. 10, pp. 3754–3765, Oct. 2012.

[35] J. Bang, J. Lee, S. Kim, and D. Hong, "An efficient relay selection strategy for random cognitive relay networks," *IEEE Trans. Wireless Commun.*, vol. 14, no. 3, pp. 1555–1566, Mar. 2015.

[36] G. Zheng, I. Krikidis, and B. Ottersten, "Full-duplex cooperative cognitive radio with transmit imperfections," *IEEE Trans. Wireless Commun.*, vol. 12, no. 5, pp. 2498–2511, May 2013.

LE THANH TAN (S'11–M'15) received the B.Eng. and M.Eng. degrees from the Ho Chi Minh City University of Technology, in 2002 and 2004, respectively, and the Ph.D. degree from the Institut National de la Recherche Scientifique–Énergie Matériaux Télécommunications, Canada, in 2015. He was a Lecturer with the Ho Chi Minh City University of Technical Education from 2002 to 2010. He is currently a Post-Doctoral Research Associate with the École Polytechnique de Montréal, Canada. His current research activities focus on Internet of Things (IoT over LTE/LTE-A network, cyber-physical systems, big data, distributed sensing, and control), time series analysis and dynamic factor models (stationary and non-stationary), wireless communications and networking, cloud-RAN, cognitive radios (software defined radio architectures, protocol design, spectrum sensing, detection, and estimation), statistical signal processing, random matrix theory, compressed sensing, and compressed sampling. He has served on TPCs of different international conferences, including the IEEE CROWNCOM, VTC, and PIMRC.

LONG BAO LE (S'04–M'07–SM'12) received the B.Eng. degree in electrical engineering from the Ho Chi Minh City University of Technology, Vietnam, in 1999, the M.Eng. degree in telecommunications from the Asian Institute of Technology, Thailand, in 2002, and the Ph.D. degree in electrical engineering from the University of Manitoba, Canada, in 2007. He was a Post-Doctoral Researcher with the Massachusetts Institute of Technology (2008–2010) and the University of Waterloo (2007–2008). Since 2010, he has been with the Institut National de la Recherche Scientifique, Université du Québec, Montréal, QC, Canada, where he is currently an Associate Professor. He has co-authored the book entitled *Radio Resource Management in Multi-Tier Cellular Wireless Networks* (Wiley, 2013). His current research interests include smart grids, cognitive radio, radio resource management, network control and optimization, and emerging enabling technologies for 5G wireless systems. He is a member of the Editorial Board of the IEEE Transactions on Wireless Communications, the IEEE Communications Surveys and Tutorials, and the IEEE Wireless Communications Letters. He has served as a Technical Program Committee Chair/Co-Chair for several IEEE conferences, including the IEEE WCNC, the IEEE VTC, and the IEEE PIMRC.